JAEA-Review
2008-002

JAEA-Review

Annual Report of R&D Activities in Center for Computational Science & e-Systems from April 1, 2006 to March 31, 2007

Center for Computational Science & e-Systems

March 2008

Japan Atomic Energy Agency

日本原子力研究開発機構

本レポートは日本原子力研究開発機構が不定期に発行する成果報告書です。
本レポートの入手並びに著作権利用に関するお問い合わせは、下記あてにお問い合わせ下さい。
なお、本レポートの全文は日本原子力研究開発機構ホームページ（http://www.jaea.go.jp/index.shtml）より発信されています。このほか財団法人原子力弘済会資料センター*では実費による複写頒布を行っております。

〒319-1195　茨城県那珂郡東海村白方白根 2 番地 4
日本原子力研究開発機構　研究技術情報部　研究技術情報課
電話 029-282-6387, Fax 029-282-5920

*〒319-1195　茨城県那珂郡東海村白方白根 2 番地 4　日本原子力研究開発機構内

This report is issued irregularly by Japan Atomic Energy Agency
Inquiries about availability and/or copyright of this report should be addressed to
Intellectual Resources Section, Intellectual Resources Department,
Japan Atomic Energy Agency
2-4 Shirakata Shirane, Tokai-mura, Naka-gun, Ibaraki-ken 319-1195 Japan
Tel +81-29-282-6387, Fax +81-29-282-5920

JAEA-Review 2008-002

Annual Report of R&D Activities in Center for Computational Science & e-Systems from April 1, 2006 to March 31, 2007

Center for Computational Science & e-Systems

Japan Atomic Energy Agency
Tokai-mura, Naka-gun, Ibaraki-ken

(Received January 8, 2008)

This report provides an overview of the research and development activities of the Center for Computational Science & e-Systems (CCSE), JAEA in fiscal year 2006 (April 1, 2006 – March 31, 2007). These research and development activities have been performed by the Simulation Technology Research and Development Office and the Computer Science Research and Development Office. The primary results of the research and development activities are the development of simulation techniques for a virtual earthquake testbed, an intelligent infrastructure for atomic energy research, computational biological disciplines to predict DNA repair function of protein, and material models for a neutron detection device, crack propagation, and gas bubble formation in nuclear fuel.

Keywords: R&D Activities, CCSE, ITBL Project, Computer Technology for Atomic Energy Research, Vibration Analysis, Grid, Computational Materials Science, Computational Quantum Bioinformatics, Vibration Analysis, DNA Repair Protein, Crack Propagation, Stress Corrosion Cracking, Superconductivity, Neutron Detection Device, Rim-Structure, Uranium Fuel, Monte Carlo Method, Finite Element Method, Molecular Dynamics, Ginzburg-Landau Model

JAEA-Review 2008-002

平成 18 年度　システム計算科学センター　研究開発年報

日本原子力研究開発機構
システム計算科学センター

（2008 年 1 月 8 日受理）

本報告書では、平成 18 年度における日本原子力研究開発機構・システム計算科学センターの研究開発活動について報告する。これらの研究開発は、高度計算科学技術開発室とシミュレーション技術開発室により執り行われた。その主な成果は、仮想振動台のためのシミュレーション技術開発、原子力研究開発のための高度インフラ整備、計算による DNA 修復機能の予測、中性子検出デバイスやき裂進展、核燃料中での気泡発生のシミュレーションに関する物性モデル開発である。

原子力科学研究所(駐在)：〒319-1195 茨城県那珂郡東海村白方白根 2-4

Contents

目　次

Acronyms

AEGIS	Atomic Energy Grid InfraStructure
ASA	Assembled Structure Analysis
API	Application Program Interface
CAEN	Computer Aided Engineering
CASC	Computer Aided Science
CARD	Computer Aided Research and Development
CCSE	Center for Computational Science & e-Systems
DNA	Deoxyribonucleic Acid
FEM	Finite Element Method
FIESTA	Finite Element Structural Analysis for Assembly
HPC	High Performance Computing
HTTR	High Temperature engineering Test Reactor
IT	Information Technology
ITBL	IT Based Laboratory
ITER	International Thermonuclear Experimental Reactor
J-PARC	Japan Proton Accelerator Research Complex
JAEA	Japan Atomic Energy Agency
JAXA	Japan Aerospace Exploration Agency
JRR-3	Japan Research Reactor No.3
JST	Japan Science and Technology Agency
LAN	Local Area Network
MEXT	Multi Experimental Tools
NAREGI	National Research Grid Initiative
NIED	National Institute foe Earth Science and Disaster Prevention
NIMS	National Institute for Materials Science
RNA	Ribonucleic Acid
SC05	Supercomputing Conference 2005
SCC	Stress Corrosion Cracking
SEM	Scanning Electron Microscope
SCUBA	Simulation Codes for Huge Biomolecular Assembly
STA	Seamless Thinking Aid

Foreword

On October 2005, The Center for Computational Science & e-Systems (CCSE) had been reorganized and R&D activities based on a five-year midterm plan have started, which include development of numerical earthquake testbed and advanced information infrastructure for atomic energy research, identification of DNA-repairing proteins, and simulation of various nuclear materials and devices.

In fiscal year 2006, which was the second year of the midterm R&D plan, these research activities have made considerable progresses. It is our pleasure to publish an annual report of these activities in fiscal year of 2006. We believe that the research and development in CCSE becomes quite fruitful through cooperative interactions with other research sections in JAEA and other organizations.

Toshio Hirayama
Director
Center for Computational Science & e-Systems,
JAEA

1. CCSE Research and Development Activities

The R&D activities of the four research teams of the JAEA CCSE are described in the following subsections. Here, we summarize the primary results of these research and development activities.

- **Computational Vibration Science for Atomic Energy Research**

Since nuclear plants are very large structures, a full-scale earthquake testbed cannot be used to evaluate their aseismic capacity. We have been developing a numerical testbed to realize virtual vibration tests of nuclear plants in supercomputers. In fiscal year 2006, we developed a computational framework for structural dynamics based on a notion called assembled structure analysis, which realizes an analysis of large structures in a part-by-part manner. The validity of the framework was tested by simulations based on large-scale datasets of actual nuclear plants. We have also developed a wave propagation simulation technique that can be used to evaluate the vibrations of both local and global structures, and proposed an improved four-node tetrahedral finite element, which enables high-quality finite-element analysis. Furthermore, as a fundamental study of aging, we have studied cavitation bubble dynamics in liquid mercury, a material which has recently been used in some nuclear facilities.

- **Fundamental Computer Technology for Atomic Energy Research**

For atomic energy research, we have developed an intelligent infrastructure “Atomic Energy Grid InfraStructure” (AEGIS), which is now used in the nuclear fusion research as the communication infrastructure for remote experiments, as well as in R&D of the virtual plant vibration simulator. We also have developed a prototype ITBL-NAREGI common client API and interoperability system that enables connection between ITBL and NAREGI.

- **Computational Quantum Bioinformatics for Atomic Energy Research**

The main cause of irradiation damage to the human body is the corruption of DNA. On the other hand, some proteins are expected to have DNA-repairing functions that reduce irradiation damage. We have been attempting to identify the proteins and their genome sequences. In the fiscal year 2006, we have developed disciplines that can predict the DNA repair function of a given protein based on computational biology. We have also developed a fast molecular dynamics simulation program for the prediction of the DNA repair function.

- **Computational Materials Science for Atomic Energy Research**

Nuclear reaction and subsequent neutron irradiation have very unique effects on materials. Since experiments to examine these effects require unusually large facilities, numerical simulations have been increasingly used to study these effects, and we have been numerically studying several effects that are crucial in atomic energy research. In fiscal year 2006, we simulated a new neutron detection device having a response speed that is much faster than that of the conventional device, and the calculated response speed was confirmed by experiments. We also developed a multiscale model that can reproduce the slow crack propagation velocity of stress corrosion cracking of metal components inside a nuclear reactor, which is the main cause of ageing, as well as a new meso-scale computer model that is capable of reproducing gas bubble formation behavior at the grain boundaries of nuclear fuel, which limits the lifetime of nuclear fuel.

1.1 Computational Vibration Science for Atomic Energy Research

1.1.1 Grid-based Large-scale Assembled Structure Analysis of an Entire Nuclear Plant Complex

The team for the development of the vibration simulator for full-scale nuclear plant is conducting R&D of large-scale simulation technologies incorporating state-of-the-art computational and IT technologies for solving the vibration dynamics of a nuclear plant in its entirety. Specifically, our attention is focused on establishing a vibration simulator on numerous supercomputers interconnected by a grid.

In order to accurately describe the behavior of an entire plant complex, it is essential to consider the interactions of the individual parts in the simulation. Thus, it is necessary to carry out numerical simulations in a part-wise manner. However, since nuclear plants are generally composed of an enormous number of parts, an extremely large dataset of parts must be processed, making simulations by conventional techniques difficult, presuming the use of a single supercomputer. To overcome this difficulty, we have established:

1. A framework that allows preparation of model data to be carried out in a part-wise manner, which guarantees high scalability, even for a large model, and allows part-connection models to be introduced into the integrated simulation of a whole plant.

2. A computing platform that enables extra large-scale whole nuclear plant simulation to be carried out on a grid computing platform called Atomic Energy Grid InfraStructure (AEGIS), which is built on high-speed interconnections of dispersed heterogeneous supercomputers.

The key technology in our R&D is assembled structure analysis (ASA). ASA is a methodology for analyzing an entire nuclear plant by heterogeneous simulations. As a first step of ASA-based R&D, we have developed a finite element implementation of ASA, called FIESTA (Finite Element Structural Analysis for Assembly), to analyze a nuclear plant as an assembled structure. In the next phase of development, we will take into consideration the actual interactions among the assembled parts. Our long-term goal is to provide advanced knowledge for engineering design, maintenance and operation of nuclear plants through detailed full-scale numerical simulations.

The developed simulation framework, FIESTA, was applied to the static and

dynamic elastic analyses of the reactor pressure vessel and cooling systems of a nuclear research facility, the High Temperature engineering Test Reactor (HTTR) at the Oarai R&D center of JAEA; see Fig. 1.1.1-1. Through such practical applications, the ASA framework, taking advantage of Grid distributed computing techniques, showed early success in describing the deformation behaviors of the major components of a nuclear plant and opened up the possibility of full-scale virtual experimentation of nuclear plants. Our research was awarded an honorable mention in the HPC Analytics Challenge held in SC05, one of the largest international conferences on high-performance computing.

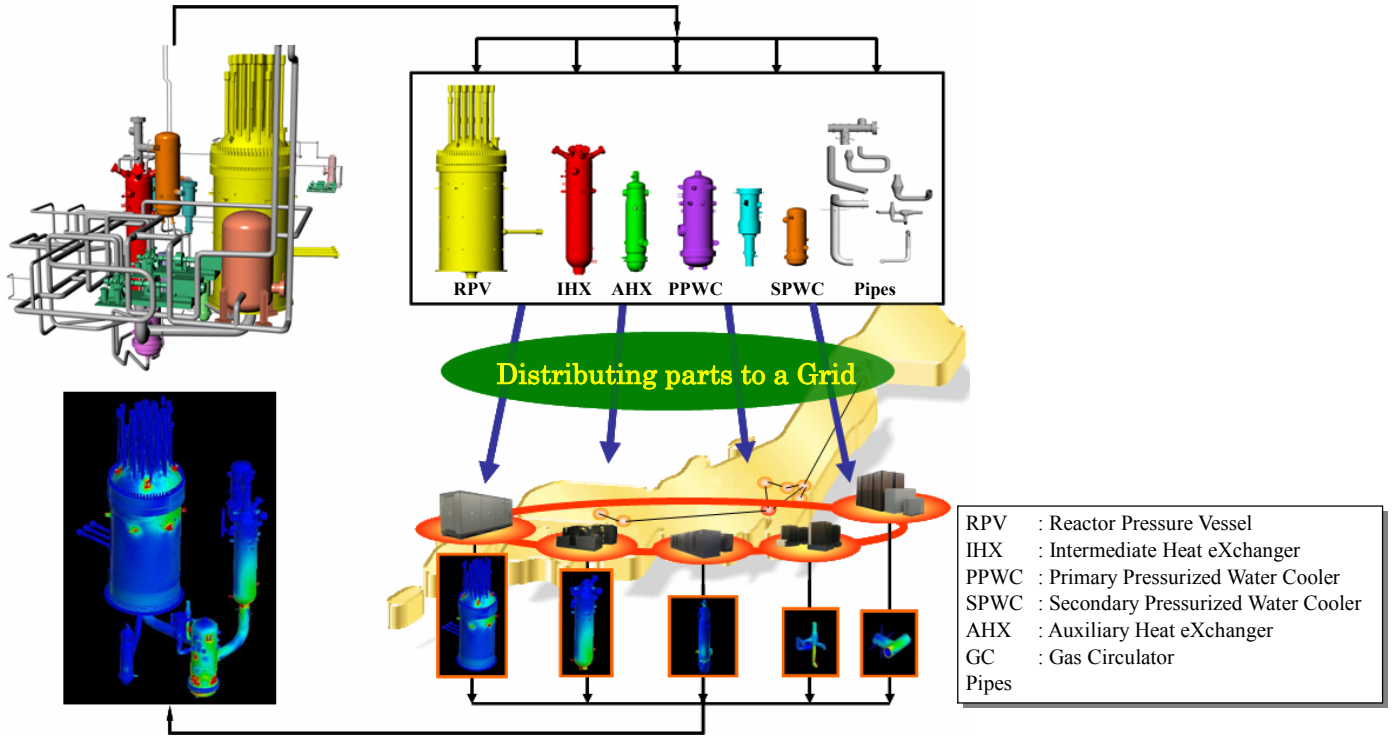

Fig. 1.1.1-1 Summary of the proposed simulation framework. A new simulation framework, called the assembled structure analysis (ASA), for analyzing an entire nuclear plant on a grid infrastructure was proposed and its first implementation based on the finite element procedures, called FIESTA, was developed. Numerical examples of the HTTR indicate that our approach would be promising in realizing the analysis of a nuclear plant in its entirety.

1.1.2 Vibration Analysis Technology to Handle a Different Wavelength

Since research and development for more reliable inspection of the safety of nuclear plants is an extremely important problem, we are cooperating with industry to examine this problem, establishing a special committee of the Atomic Energy Society of Japan. To solve this problem, a maintenance management experiment or an aging inspection experiment using an actual nuclear reactor or a nuclear plant under real conditions in a real environment is necessary. However, this type of experiment has the disadvantages of high cost and time requirements, and hence, it is not easy to perform such experiments. Therefore, at the Center for Computational Science and e-systems, we began a trial of a safe and effective safety evaluation of a nuclear plant employing computational science technology. As the first step, we are tackling the issue of research and development of simulation of the three-dimensional vibration of an entire nuclear plant, which cannot be achieved using an experimental vibration table.

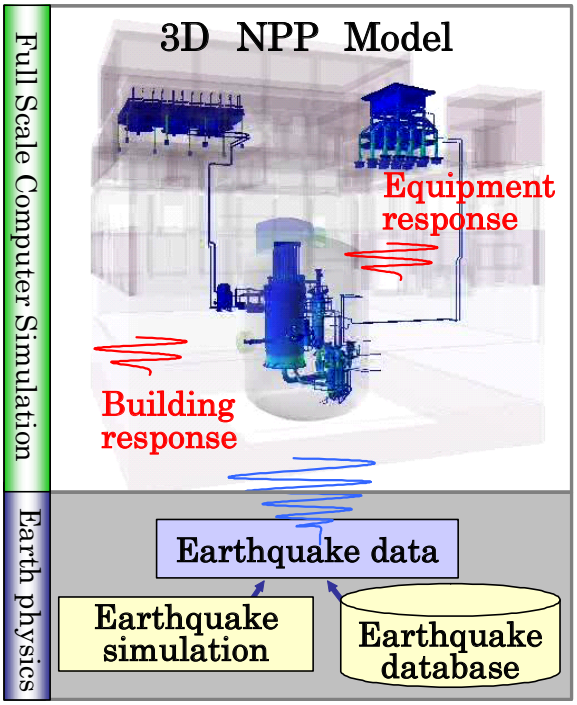

Fig. 1.1.2-1 Vibration simulator for a full-scale nuclear plant. We are developing a technology to enable the reproduction of various phenomena in nuclear plants by using a three-dimensional numerical model of an entire plant in a computer system.

This technology, referred to as the vibration simulator for a full-scale nuclear plant, digitizes a three-dimensional model of an entire nuclear plant in a computer and enables the simulation of various phenomena that occur in a nuclear plant by combining conventional technologies related to earthquake and ground motions. The calculation of the resonances of a complicated structure with high precision through vibration analysis is a critical technology that is required in order to realize this vibration simulator for the full-scale nuclear plant.

In the resonance phenomenon, the vibration energy of earthquakes is transmitted as a wave in a structure, leading to the reflection and transmission of the wave at connections, which are points of discontinuity. This phenomenon repeats itself at several connections, and the structure is shaken strongly where the energy is concentrated and the vibration is amplified. Resonance is generated over a wide frequency range that varies from the vibrations of the entire structure to some local vibrations of a structural component. Furthermore, in the worst-case scenario, the resonance may lead to the collapse of the structure within a few seconds. The goal of the present study is therefore to improve the safety of nuclear plants by analyzing the resonance state through computational science technology and to provide solutions for the reduction of resonance in a complicated structure.

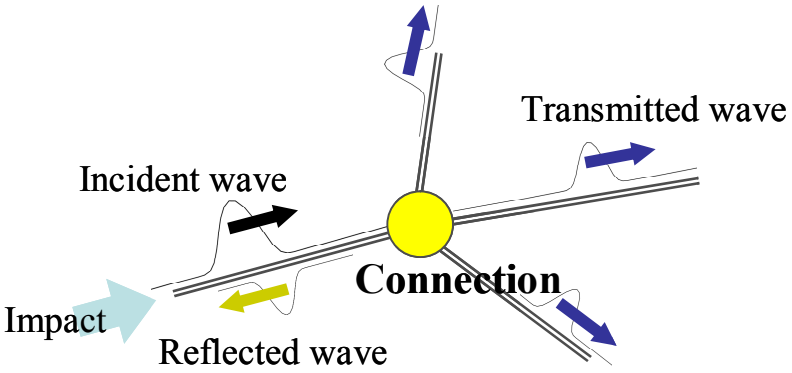

Fig. 1.1.2-2 Wave reflections and transmissions at a connection. The repetition of reflections and transmissions of the wave, which are generated at points of discontinuity, such as connections, contribute to the vibration phenomenon of the structure. The simulation of these waves enables the development of a vibration reduction plan and preventive measures against vibration.

It is possible to evaluate the problem of resonance of vibrations in an entire structure by conventional computational science technology. However, local structural vibration cannot be evaluated with sufficient precision because the reflected wave cannot be sufficiently modeled by conventional technology. Therefore, we attempted to develop a wave propagation simulation technique that can evaluate the vibrations of local structures as well as those of entire structures. The proposed technique was applied to a piping structure and was successful in simultaneously treating vibrations in both the entire structure and the local structure. This technique can be applied to an actual nuclear plant. As a result, it can be used to calculate the resonances of a complex structure with high precision and provide solutions for reducing them.

1.1.3 Development of highly accurate four-node tetrahedra with rotational dofs

With the developments in architectural engineering and mechanical design, three-dimensional simulations with high accuracy at a lower cost become increasingly important in the structural engineering field. Because of their suitability for arbitrarily complex geometries and fully automatic mesh generations, four-node tetrahedral elements are indispensable to complex finite element structural analysis, for example, the simulation of an entire nuclear plant.

In the present study, we have investigated the accuracy of the newly developed four-node tetrahedra, RGNTet4 and GNTet4, by comparison with existing finite elements. Among the existing elements used in the comparative study, TET4RX and HT4R are advanced and favorable for the four-node tetrahedra installed in ANSYS®, a commercial finite element analysis code. These two tetrahedra were proposed by improving a conventional four-node tetrahedron (Tet4) with the aid of rotational parameters implemented by extremely complex formulations. The accuracy of these tetrahedra was demonstrated to be significantly better than Tet4 equipped with only translational degrees of freedom (dofs). These tetrahedra, however, fare poorly in terms of accuracy with respect to the conventional 10-node tetrahedron (Tet10).

RGNTet4 and GNTet4 are tetrahedra that we proposed recently based on the partition of unity method, by which the continuity of displacement between element boundaries and the implementation of higher-order displacement fields are guaranteed. Both of the newly developed tetrahedra, as well as TET4RX and HT4R, contain rotational dofs, which are known as an important parameter for accuracy, and use only corner nodes. Using the proposed tetrahedra, all spurious zero-energy modes that lead to non-physical deformation can be suppressed naturally, and no stabilization techniques or parameters are required. Furthermore, compared with the existing tetrahedra TET4RX and HT4R, the proposed tetrahedra are much more straightforward in formulation.

Although the four tetrahedra mentioned above are all equipped with rotational dofs, they are based on different implementations of rotational dofs, and the effects of the dofs on accuracy are not yet fully understood. We have therefore attempted to perform a comparative study focusing on the accuracy and formulations of the four tetrahedra.

Let us discuss the accuracy of the proposed tetrahedra using simple examples. Figure 1.1.3-1 shows a curved cantilever beam subjected to a unit in-plane force P_1 and a unit out-of-plane force P_0 at the free end. All of the displacements at the clamped end

are restrained. The results, including those for Tet4, Tet10, and the conventional eight-node hexahedron (Hex8) for reference, are summarized in Table 1. TET4RX and HT4R outperform the displacement-based tetrahedron RGNTet4, but their accuracy is dependent on the penalty parameter. Furthermore, TET4RX, HT4R, and RGNT4 significantly surpass the low-order elements Tet4 and Hex8 in accuracy, but are inferior to Tet10. In contrast, GNTet4 has a performance that is equivalent to that of Tet10 and is better than the performances of the other elements.

The convergence of the L_2 norms of the error in displacement and energy is studied for the cantilever beam problem illustrated in Figure 1.1.3-2. The problem domain is decomposed into cubic blocks, which are subsequently divided into tetrahedra as shown in Figure 1.1.3-2. The boundary conditions are set as shown in Figure 1.1.3-2. Figures 1.1.3-3(a) and 1.1.3-3(b) show the convergence plots of the L_2 norms of the error in displacement and energy, respectively. GNTet4 shows the typical convergence behaviors of the conventional quadratic tetrahedron Tet10. RGNTet4 has a convergence rate between that of Tet10 and that of Tet4. RGNTet4 and GNTet4 have the expected convergence properties, namely, the convergence of GNTet4 is of quadratic order, while that of RGNTet4 is of an order between linear and quadratic.

In the present study, we have reported that

(1) GNTet4 and RGNTet4 are not parameter-dependent, require no special stabilization, and are straightforward in formulation;

(2) GNTet4 and RGNTet4 significantly surpass the conventional elements Tet4 and Hex8 in accuracy, although they have extremely simple formulations;

(3) GNTet4, RGNTet4, and Tet4 use the same mesh and are consistent in formulation and computer implementation.

In the future, the newly proposed elements might allow us to accurately simulate the behavior of an entire nuclear plant.

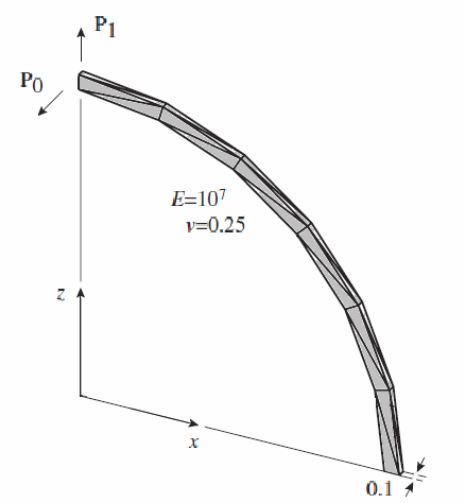

Figure 1.1.3-1 Curved beam subjected to a unit force.

Table 1 Numerical results for the curved beam normalized by the theoretical solutions.

Element	In-loading P_1	Out-loading P_0
Tet4	0.023	0.005
Tet10	0.716	0.796
Hex8	0.060	0.188
TET4RX(γ =1e-6)	0.184	0.690
TET4RX(γ =1)	0.040	0.072
HT4R(γ =1e-6)	0.140	0.269
HT4R(γ =1)	0.134	0.235
RGNTet4	**0.196**	**0.204**
GNTet4	**0.974**	**0.900**

The theoretical solutions:
0.08734 for loading P_1 and 0.50220 for loading P_0
γ : Penalty parameter

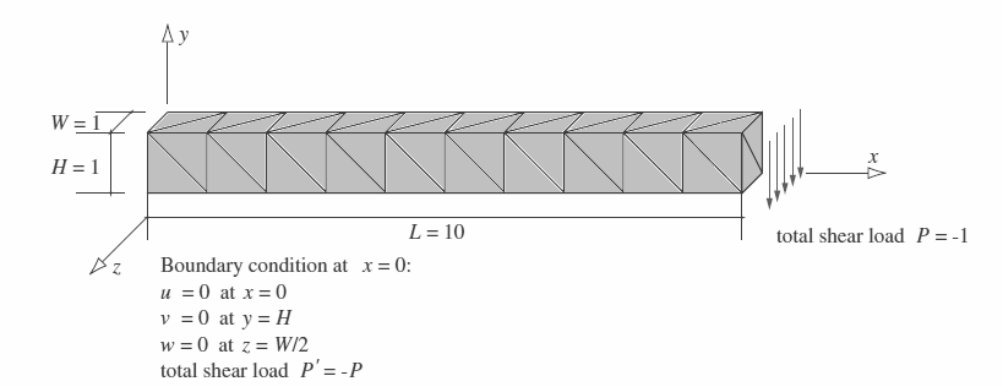

Figure 1.1.3-2 Cantilever benchmark problem used in the convergence study.

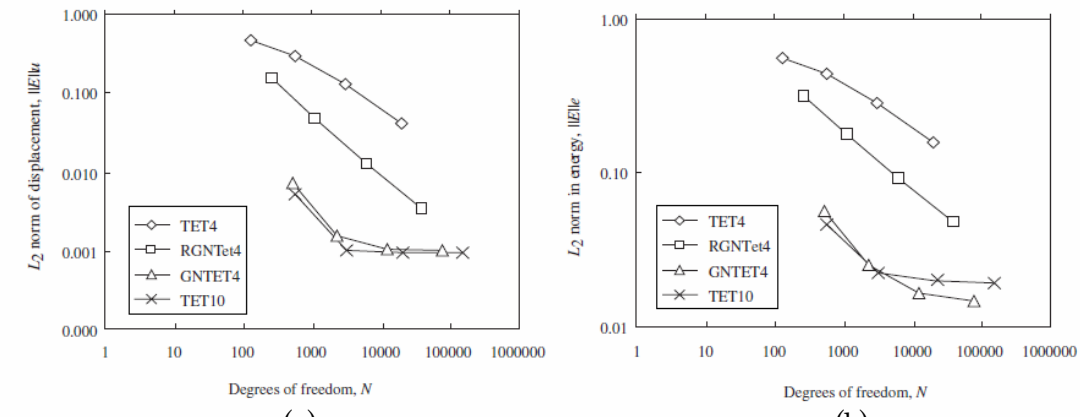

Figure 1.1.3-3 Convergence plots for the cantilever problem: L_2 error norms of (a) displacement and (b) energy.

1.1.4 Numerical study of cavitation bubbles in liquid mercury

Cavitation in liquids, which causes damage (i.e., cavitation erosion) to solid surfaces and sometimes seriously shortens the lifetime of structural components, is a crucial issue in many hydraulic machines. When cavitation occurs in a liquid, many vapor or gas-vapor bubbles, called cavitation bubbles, emerge in the liquid and emit a high-speed liquid jet toward nearby solid surfaces causing cavitation erosion. The same problem has been encountered in the field of nuclear science and engineering. Cavitation in water has sometimes caused the destruction of pipes in nuclear power plants, and cavitation in liquid mercury poses a serious problem in the development of the accelerator system at the Japan Proton Accelerator Research Complex (J-PARC).

In the Materials and Life Science Experimental Facility of J-PARC, liquid mercury is used as the material for the spallation neutron source, in which flowing liquid mercury is bombarded by pulsed proton beams to produce intense neutron fluxes. Based on experimental investigations performed at J-PARC, it has been suggested that, at the moment of bombardment, high-intensity pressure waves are radiated due to an enormous amount of energy release and that these waves would cause cavitation when propagating in the mercury. Recently, it was predicted that the cavitation will significantly reduce the lifetime of the target vessel. The current estimation of the lifetime is only approximately 30 hours, although the previous estimation, determined based on radiation embrittlement, was more than 2,500 hours. Thus, a method by which to predict and suppress cavitation events is now strongly desired.

We have investigated numerically the dynamics of cavitation bubbles in liquid mercury in order to clarify their characteristics. While a large number of studies have examined cavitation in water, there have been very few studies on cavitation bubbles in liquid mercury. Therefore, an analysis of the fundamental characteristics of cavitation bubbles in liquid mercury is necessary. In the present study, we focused primarily on the expansion velocity of cavitation bubbles under negative pressure, which is strongly correlated with the erosion intensity of the bubbles. The theoretical model used in the numerical study is a Rayleigh-Plesset type nonlinear equation that takes into account the interaction between bubbles through the pressure waves that the bubbles radiate when they expand. This model describes the radial motion of interacting spherical bubbles. Figure 1.1.4-1(a) shows the pressure change in liquid mercury measured at J-PARC, which was used in our study as the driving force of bubble dynamics. The solid lines in Fig. 1.1.4-1(b) show an example of the numerical results, in which the interaction of two cavitation bubbles of small initial radii (15 μm and 10 μm) was considered. The

thick lines denote the multibubble cases, and the thin lines denote the single-bubble cases, in which bubble-bubble interaction is neglected. In the negative-pressure period, the bubbles expand explosively, which implies the occurrence of cavitation inception. Compared to the single-bubble cases, the expansion velocity in the multibubble case is closer to the experimental data (denoted by the symbols in the same figure), suggesting that bubble-bubble interaction is responsible for determining the expansion velocity of cavitation bubbles. The quantitative discrepancy in the multibubble case might be due to many-bubble effects or an experimental uncertainty caused by the opacity of mercury.

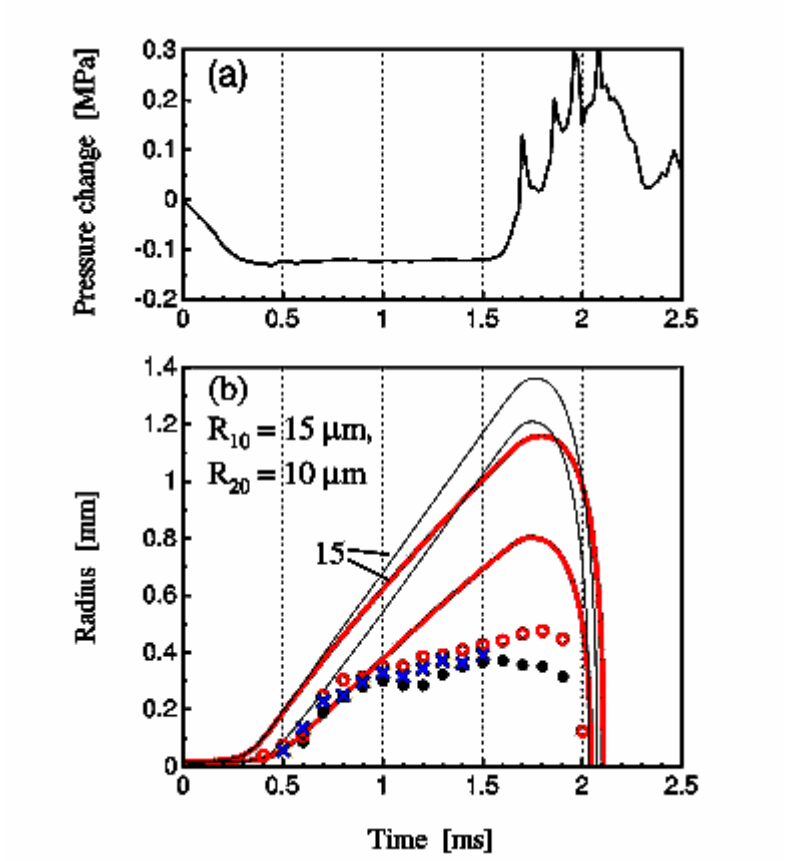

Fig. 1.1.4-1 (a) Measured pressure change in liquid mercury and (b) radius-time curves obtained experimentally (symbols) and numerically (lines). In (b), the thin lines and the thick lines are for the single-bubble and double-bubble cases, respectively. The initial radii of the bubbles are 15 μm and 10 μm. The number shown in (b) indicates the initial radius (μm) of the corresponding bubble.

The numerical results shown above suggest that the expansion velocity is decreased by bubble-bubble interaction and is time-dependent in multibubble cases even after the bubble expansion has converged to a quasi steady state. We have proposed a simple theory to explain this numerical finding. Figure 1.1.4-2 shows the expansion velocity of isolated and two interacting bubbles having initial radii of 10 μm. The results obtained by the proposed theory (dashed lines) are in reasonable quantitative agreement with the full numerical simulation (solid lines) when the bubble expansion is in the (quasi) steady state. In addition, the theory accurately describes the time dependence of the expansion velocity in multibubble cases.

As discussed above, the proposed theory provides an accurate prediction of the expansion velocity, which has a strong correlation with the erosion intensity of cavitation bubbles. The above-mentioned findings and the theory are now used in the development of cavitation suppression technology based on gas bubble injection, in which the interaction of cavitation bubbles with gas bubbles injected into liquid mercury plays a crucial role [1.1.4-2].

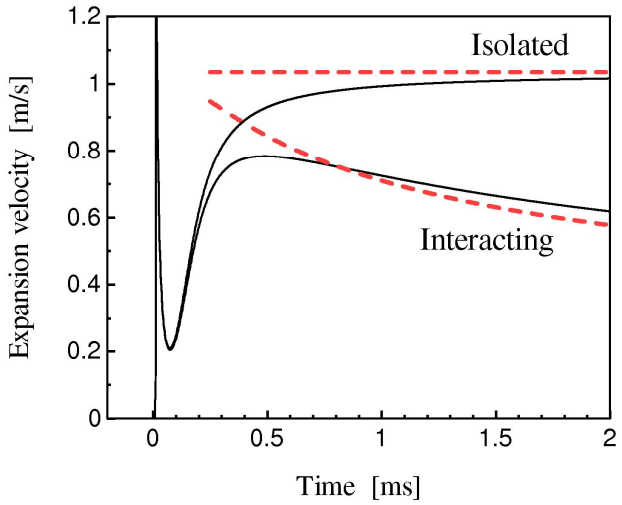

Fig. 1.1.4-2 Expansion velocity of an isolated bubble and two interacting bubbles, each having an initial radius of 10 μm. The solid lines denote the results of full numerical simulation, and the dashed lines denote the asymptotic values given by the proposed theory.

References

[1.1.1-1] A. Nishida, H. Matsubara, R. Tian, O. Hazama, Y. Suzuki, F. Araya, N. Nakajima, M. Tani, and M. Kondo, "Numerical simulation system "Three-dimensional virtual plant vibration simulator" for nuclear plants by using assembled structural analysis," Trans. At. Energy Soc. Japan **6**, 376 (2007) [in Japanese].

[1.1.2-1] Akemi Nishida, "Wave Propagation Properties of Frame Structures - Formulation for Three-Dimensional Frame Structures," JSME International Journal Series B **49** (*Special Issue on International Conferences on Power and Energy*), 360 (2006).

[1.1.3-1] Rong Tian, Hitoshi Matsubara and Genki Yagawa, "Advanced 4-node tetrahedrons," Int. J. Numer. Meth. Engng. **68**, 1209 (2006).

[1.1.4-1] M. Ida, T. Naoe, and M. Futakawa, "Direct observation and theoretical study of cavitation bubbles in liquid mercury," Phys. Rev. E **75**, 046304 (2007).

[1.1.4-2] M. Ida, T. Naoe, and M. Futakawa, "Suppression of cavitation inception by gas bubble injection: A numerical study focusing on bubble-bubble interaction," Phys. Rev. E **76**, 046309 (2007).

1.2 Fundamental Computer Technology for Atomic Energy Research

1.2.1 Research and Development of Atomic Energy Grid InfraStructure: AEGIS

The Center for Computational Science and e-systems of the Japan Atomic Energy Agency (CCSE/JAEA) has launched a new study on the Atomic Energy Grid InfraStructure (AEGIS). The objective is to construct an intelligent infrastructure for atomic energy research to enable synchronization of three themes:

1) Computer-Aided Research and Development (CARD)
   to realize an environment for seamless thinking aid (STA)
2) Computer-Aided Engineering (CAEN)
   to establish multi experimental tools (MEXT)
3) Computer Aided Science (CASC)
   to promote the atomic energy research and investigation (AERI)

R&D on the network computing system for the atomic energy field is an attempt to construct a system that corresponds to the base of AEGIS using the knowledge and skills of the ITBL (Information Technology Based Laboratory) national project, which is an e-Japan priority plan. It is important to ensure the safety, certainty, and reliability of this system for large-scale facilities and supercomputers in the field of atomic energy research through the Internet. Therefore, we have improved the communication infrastructure developed in ITBL to provide secure communication through the Internet and have developed more reliable communication middleware. The improved communication infrastructure is currently being used as the communication infrastructure for remote experiments in nuclear fusion. In addition, the improved communication infrastructure is used for the three-dimensional virtual plant vibration simulator.

In addition, we have implemented a digital certificate to improve security for accessing the Local Area Network (LAN) of JAEA from the internet and have installed file servers and TV meeting systems. The system allows users to share information among certificated users. We are currently engaged in collaborative R&D with not only Japanese universities and institutions but also German, French, and American nuclear and computational agencies, for the further development of computational science and information technology in the field of atomic energy research.

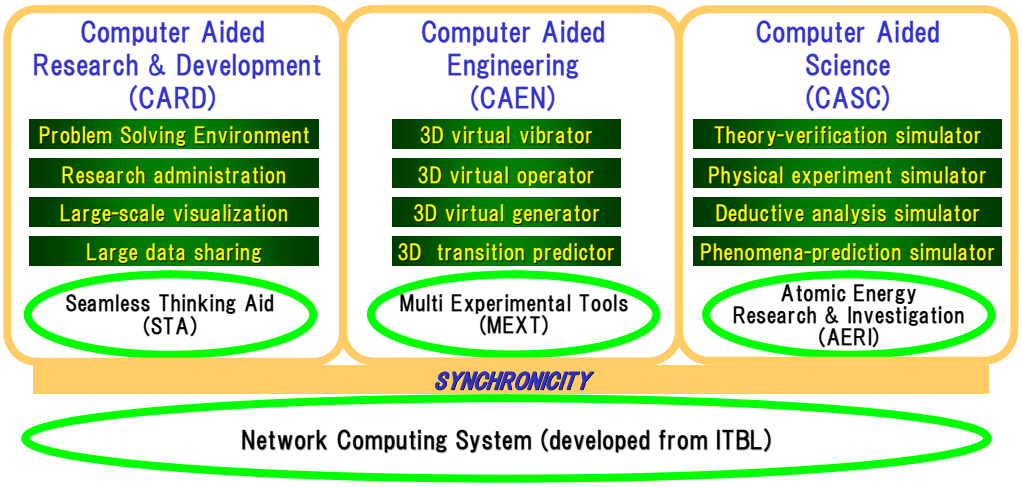

Fig.1.2.1-1 Concept of AEGIS

1.2.2 Japanese national project on “Development and Applications of Advanced High-performance Supercomputer”

In Fiscal Year 2006, the Ministry of Education, Culture, Sports, Science and Technology launched a national project called the “Development and Applications of Advanced High-Performance Supercomputer” to establish a next-generation supercomputer system. The CCSE is involved in this project and is engaged in R&D of grid middleware. The objective of this R&D is to establish an infrastructure that allows smooth transition of technology and know-how in the Information Technology Based Laboratory project to the next-generation national grid infrastructure in Japan.

The ITBL project is a national project that belongs to the e-Japan Priority Policy Program to realize the e-Japan Strategy, which sets goals to make Japan the world's most advanced IT nation. The ITBL project was launched in April of 2001 by six institutes, namely, NIMS, NIED, JAXA, RIKEN, JST, and JAEA, and was continued until March of 2006 as a five-year plan. The objective of the ITBL project is to establish virtual laboratories in which researchers engaged in various disciplines can collaboratively develop highly sophisticated simulation systems by fully utilizing the computer resources of a high-speed network. The ITBL grid infrastructure has been operated continuously since the completion of the ITBL project and made available 74 TFlops of computer resources at the end of the Fiscal Year 2006.

To achieve the next-generation national grid infrastructure, CCSE aims to develop the following two middleware packages:

1) A common client API for ITBL and National Research Grid Initiative

The National Research Grid Initiative (NAREGI) is a project to research and develop practical grid middleware according to global standards, so that a large-scale computing environment (the Science Grid) can be implemented for widely distributed, advanced research and education. Using a common client API, users are able to access both environments without changing their applications. Our goal is to construct a common client API that is applicable to various grid computing environments.

2) A connection between ITBL and NAREGI

Through this connection, users are able to execute jobs, access files, and obtain resource information from their original environment.

In Fiscal Year 2006, we demonstrated several applications implemented by the prototype ITBL-NAREGI common client API that we have developed. Furthermore, we designed an interoperability system that enables connection between ITBL and

NAREGI.

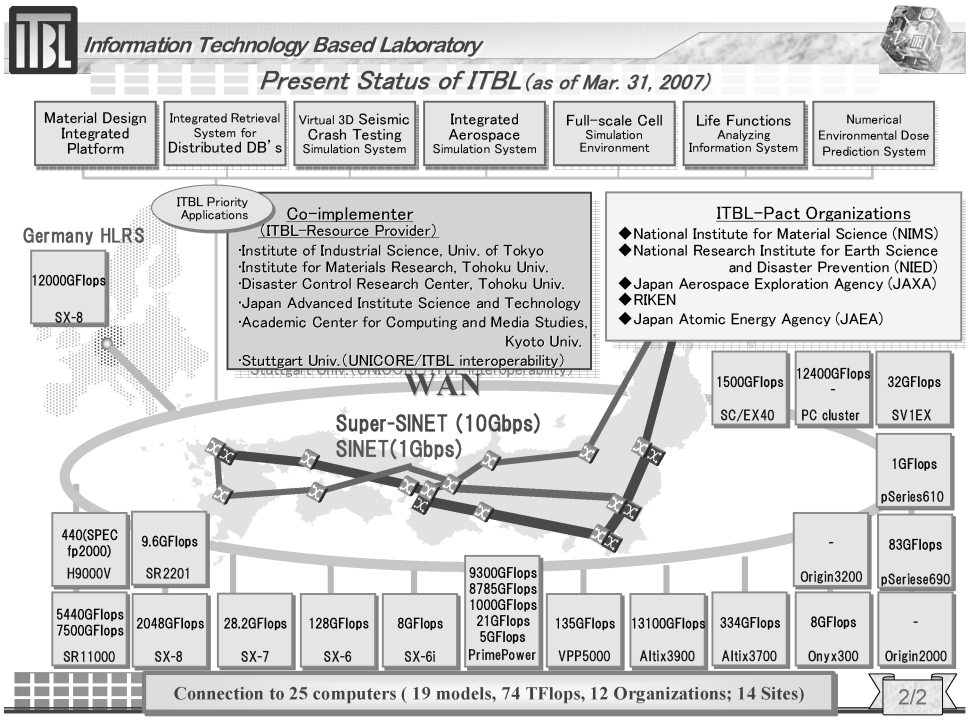

Fig.1.2.2-1 Status of ITBL

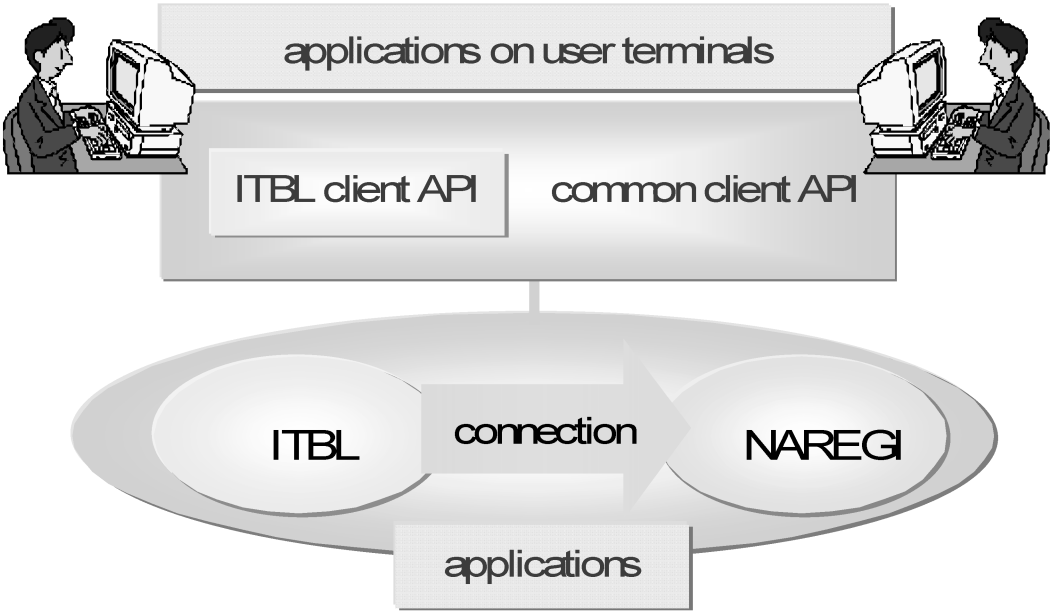

Fig.1.2.2-2 Toward the next-generation national grid infrastructure in Japan

1.3 Computational Quantum Bioinformatics for Atomic Energy Research

1.3.1 Computational Predictions of DNA Repair Related Genes/Proteins Based on Genome Databases

Organisms are under constant exposure to radiation, including ultraviolet light. Irradiating intense light on organisms can break the chemical bonds of DNA strands or alter the chemical structure of DNA bases. Such damage is considered to be one of the causes of cancer and ageing. In order to undo such damage, organisms have mechanisms to automatically detect and repair damaged DNA. Molecular mechanisms for DNA repair have attracted a great deal of attention, and extensive studies have been carried out.

We have been investigating the molecular mechanisms of DNA repair by identifying genes for DNA repair from entire genome sequences and by simulating dynamic structures of proteins at the time they repair DNA. Although the genome sequences of several organisms are known now, all of the genes related to DNA repair have not yet been identified. Genome sequences are equivalent to a string of letters written with only four types of characters, and methods to decipher this string are still under development in laboratories all over the world. The process of deciphering genome sequences involves collaboration between biological and computational sciences, and this new field is called bioinformatics. The bioinformatics research described herein relates to an attempt to identify DNA repair related proteins.

In fiscal year 2006, we used our preliminary databases and applied deciphering methods to predict the biological functions of proteins deduced from genome sequences. This research was performed in collaboration with the Graduate School of Science, Nagoya University.

Photolyase, a protein to repair DNA damaged by ultraviolet light, is encoded by a gene in a huge gene family called the photolyase-blue-light-photoreceptor family, and all of the proteins encoded in the genes of the family have similar amino acid sequences due to the fact that they are derived from a common ancestor. We extracted all of the genes related to photolyase from our DNA repair protein database and constructed a phylogenetic tree (Figure 1.3.1-1). It is relatively easy to find amino acid sequence similarity among these proteins, but it is unclear as to whether these proteins are actually capable of repairing DNA damaged by ultraviolet light. Gene products in this

family are known to have one of the functions for repairing cyclobutane pyrimidine dimer (CPD), binding a single-strand DNA, dealing with the biological clock, and repairing the 6-4 product of DNA. These functions are broadly related to intense light, but the type of output of the activity is diverse. Biochemical function assay has been the only method by which to verify the function of the gene products. The assay experiments to determine the function of a protein are laborious, and it is practically impossible to perform experiments on all the proteins. Computational biology provides the opportunity to narrow down the range of possible functions among the proteins predicted from the genome sequences and thereby accelerate the biochemical assay.

We have performed quantum mechanical calculations to analyze the electron transfer reaction from the small molecule excited by ultraviolet light included in photolyase to the damaged DNA using the three-dimensional structure of *Anacystis nidulans* photolyase with the supercomputer in JAEA and found that there were two major electron pathways that reached the damaged DNA. One of these pathways is a direct route from the small molecule to the damaged DNA, and the other route is via the methionine residue at site 353 (Met353). Both pathways had a similar current of electrons, and we concluded that both pathways were important for the protein to function as a DNA repair enzyme.

The quantum mechanical calculations suggest that Met353 is a good indicator for predicting functions based on amino acid sequences. To support this idea, we analyzed the concerted conservation of amino acid residues in homologous 371 amino acid sequences belonging to the photolyase-blue-light-photoreceptor family. When these sequences were divided into two groups based on the indicator, 201 sequences were found to have methionine at a site homologous to 353 of *A. nidulans* photolyase, and 170 sequences were found to have other types of amino acid at this site. We found 12 more amino acid residue sites that behaved in a manner similar to the residue at 353 during the molecular evolution. Each of these sites was conserved in the 201 sequences, but mutated to different types of amino acid residue in the 170 sequences (Figure 1.3.1-2). These residues were found to be located between the small molecule and the damaged DNA bound to the enzyme (Figure 1.3.1-3). Met353 was found to be the key residues for electron transfer, and presumably the other 12 residues play a role in maintaining the pathway. The results obtained from two different disciplines of computational biology strongly suggest that these 13 residues are good markers for predicting the DNA repair functions of the protein in the family based on amino acid sequences, and the 201 sequences that were found to have methionine at a site homologous to 353 of *A. nidulans* photolyase are predicted to have DNA repair activity,

while the 170 sequences that were found to have other types of amino acid are predicted to be incapable of repairing CPD damage of DNA.

We cross-validated our predictions with the available biochemical analysis and found that the predictions were correct in 24 cases. Only 25 biochemical function validation experiments have been reported thus far, and only one case contradicted our analyses. The one contradictory case is a functional annotation given to the amino acid sequence derived from mustard (PHR1_SINAL in Figure 1.3.1-2). We predicted that the function of the sequence is non-DNA repair based on our calculation, yet it is reported as CPD photolyase. We suggested that the function of the protein was controversial, and the annotation in the international database is actually debatable in the field.

The above-described study demonstrated that computational and experimental biology research are a good combination for annotating genome sequences, and we will continue to develop databases and methods to annotate genes/proteins related to DNA repair.

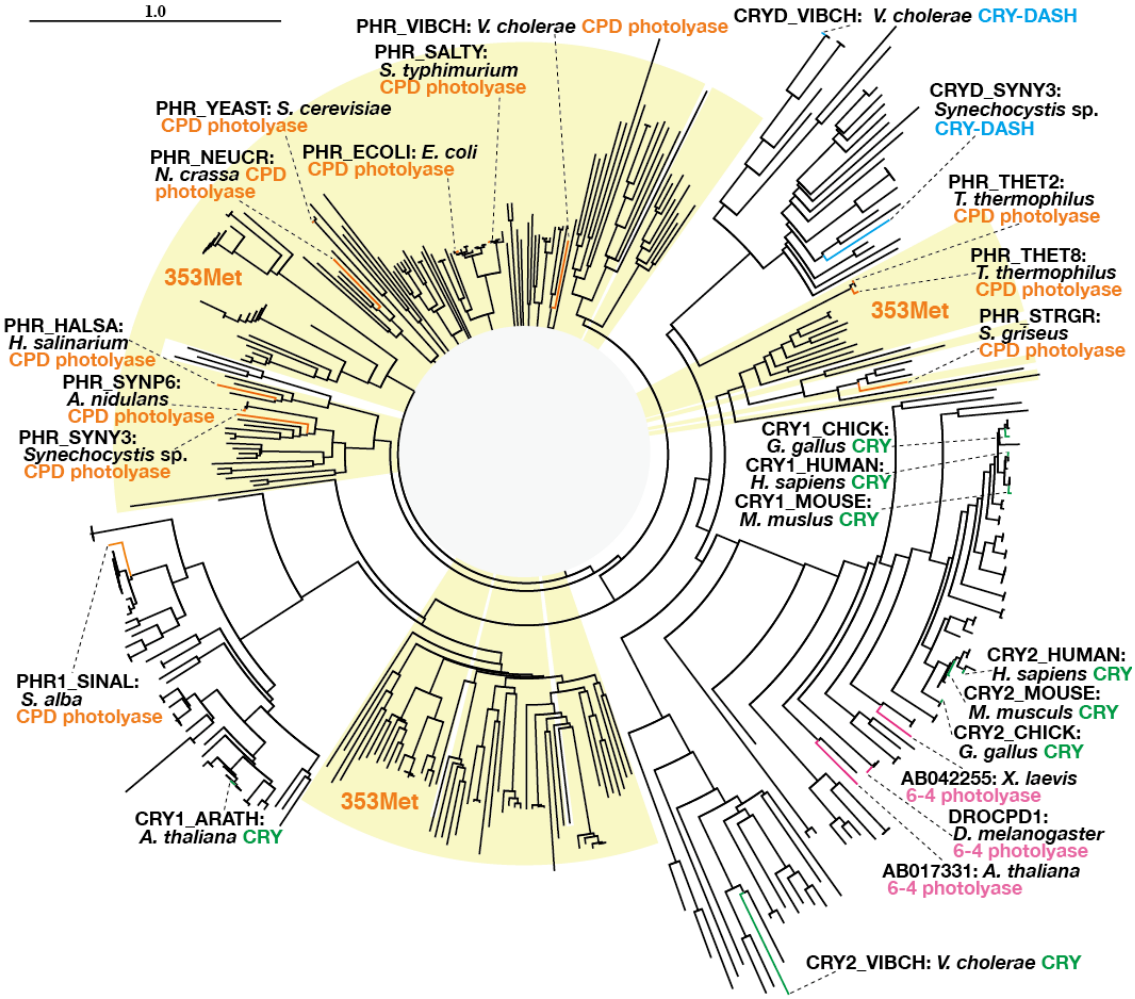

Fig. 1.3.1-1. Dendrogram of proteins belonging to photolyase-blue-light-photoreceptor family. The tree was drawn based on the neighbor-joining method, and the distance matrix was calculated based on Kimura's distance. The distance is proportional to the evolutionary distance. The length of one amino acid substitution per site is indicated at the top left. Although the tree is supposed to start at the center of the figure, the center of the tree and the branching order around the center cannot be located without statistical ambiguity due to the paucity of data. Therefore, the center area is covered by a grey circle. The yellow background indicates that the amino acid residue that corresponds evolutionarily to the 353rd amino acid residue in the protein from *A. nidulans* is methionine. See the text for the details. Colored branches indicate that the biological function of the proteins is tested biochemically. Orange indicates a protein has an activity to repair cyclobutane pyrimidine dimer (CPD). Cyan indicates a protein that has single-strand DNA binding activity. Blue indicates a protein that has a function related to the biological clock. Purple indicates a protein that has an activity to repair the 6-4 product. Note that PHR1_SINAL (bottom left) derived from mustard is annotated as

CPD photolyase, yet our analyses demonstrated that the protein should be related to the biological clock.

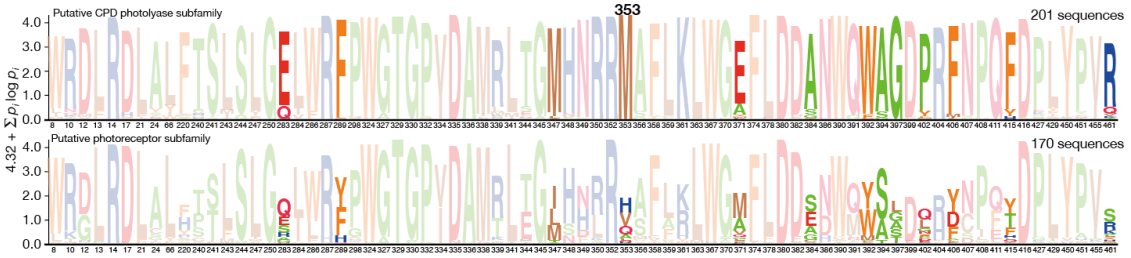

Fig. 1.3.1-2: Two types of amino acid residue conservation pattern obtained by focusing on the residue type at 353. The upper conservation pattern is from the putative CPD photolyase subfamily (201 amino acid sequences), and the lower pattern is from the putative photoreceptor subfamily (170 sequences). The distinction was made based on the type of residue at 353. The horizontal axis is the residue number from *A. nidulans*, and the vertical axis is the information entropy subtracted from the constant value of 4.32. Each site is depicted by types of residue, and the occupancy of each residue type is depicted by the height of each residue. The perfectly conserved site has a value of 4.32 with a single amino acid type, and the completely random site has a value of zero. The sites indicated by translucent colors are sites for which the conservation patterns are the same in both families, and sites indicated by solid colors are sites for which the conservation patterns are different between the two families, suggesting that the sites are determinant for each biological function.

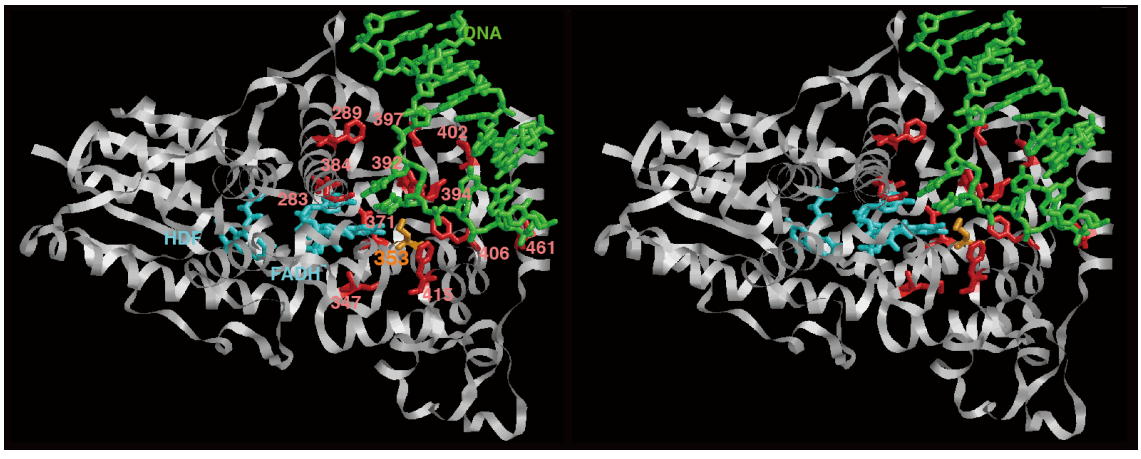

Fig. 1.3.1-3: Spatial location of amino acid residues with unique conservation patterns. The protein (white ribbon) with DNA (green stick) is shown in a stereo figure. Red residues have a unique conservation pattern in each family, as shown in Figure

1.3.1-2. Molecules shown in cyan are co-factors that receive ultraviolet light and emit electrons to DNA. Note that the red residues are all located in the pathway between the molecules shown in cyan and DNA.

1.3.2 Fast Molecular Dynamics Simulation Programs for Studying Repair Mechanisms of Damaged DNA

Molecular dynamics (MD) simulation not only provides dynamic descriptions of molecules on the atomic scale, but also provides valuable information for the interpretation of experimental data. The rapid development of faster computers and the elucidation of the structures of biological macromolecules by X-ray crystallography and other experiments have enabled us to perform large-scale MD simulations of large biological molecules.

We are developing an integrated molecular simulation system for biological macromolecules, called SCUBA (Simulation Codes for hUge Biomolecular Assembly), which is designed to efficiently run a system composed of more than a million particles on parallel computers. SCUBA has many special features, several of which are listed below.

- High performance
  By intensive parallelization and vectorization, and by using the dynamic load balance mentioned in 10, 11, and 12, SCUBA has achieved both a high parallelization efficiency ratio and a high vectorization ratio. On the Earth Simulator, SCUBA has achieved a parallelization efficiency ratio of 75.8% and a vectorization ratio of 96.2%, and 45 nodes (360 processors) were used to perform an MD simulation for a system of the RuvAB-Holliday junction complex, consisting of 546,725 atoms, in Fig. 1.3.2-1.
- Parallelization
  SCUBA employs the domain decomposition (DD) method, which divides the volume of the physical system into rectangular subcells with lengths longer than the potential cutoff radius. In the conventional DD method, each processor needs to evaluate the interactions between atoms in a cell and the surrounding 26 neighboring cells. SCUBA employs a method for minimizing communication between processors, in which each processor evaluates the interactions of atoms with only seven surrounding cells.
- Vectorization
  In order to improve the performance of SCUBA, the algorithm to calculate the interactions among the atoms is intensively vectorized.
- Dynamic load balance
  A dynamic load-balancing algorithm is implemented to optimize the number of processors assigned for several different types of calculation during the simulations.

This fiscal year, the arrays used in the SCUBA program were intensively optimized

to reduce the amount of memory use. This optimization enabled SCUBA to perform molecular dynamics simulations of large-scale supra-molecular systems comprised of more than one million atoms. We have carried out a benchmark test of SCUBA. The physical system chosen for this test was ribosome, a supra-biomolecular complex, consisting of four RNA molecules and approximately fifty protein molecules. Ribosome is one of the supra-biomolecules working in the process of translating genetic information to polypeptides. The size of the 70S ribosome system and the number of atoms in the system are 286 A × 286 A× 263 A and 1,878,425 atoms, respectively. SCUBA achieved a parallelization efficiency ratio of 81.6 %, even when 512 processors were used on Altix3700Bx2 computer, as shown in Fig. 1.3.2-1.
Part of the numerical calculations were carried out on Earth Simulator in the Earth Simulator Center.

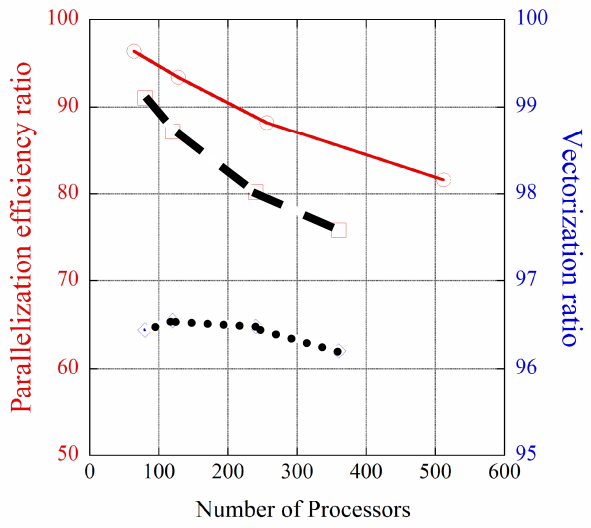

Fig.1.3.2-1. Performance of SCUBA
The parallelization efficiency ratio and vectorization ratio performance of the Earth Simulator are indicated in dashed and dotted lines, respectively. (The system of the RuvAB protein – Holliday junction DNA complex consists of 546,725 atoms.) The parallelization efficiency ratio performed on an Altix 3700Bx2 computer is indicated by the solid line. (The system of ribosome consists of 1,878,425 atoms.)

Reference:

[1.3.1-1] Miyazawa, Y., Nishioka, H., Yura, K., Yamato, T. (2007/2008) Discrimination of class I CPD photolyase from blue light photoreceptors by single methionine residue. *Biophysical Journal*, in press.

1.4 Computational Materials Science for Atomic Energy Research

1.4.1 Prediction of the Response Time of Superconducting MgB_2 Neutron Detector

A highly accurate irradiation detector can be constructed by taking advantage of the properties of a superconductor, the electrical resistance of which abruptly goes to zero at the superconducting transition temperature. The reason for this is that even the tiny heat created by one radiation particle brings about a large electrical signal in superconductors. In fact, the superconducting radiation detector is now utilized as an essential detector for X- and γ-rays in astrophysics to study the origin and development of the universe. Moreover, its ability to count only a single photon and identify a very small amount of actinide compound is considered to be quite useful in future quantum communication and microanalysis of nuclear materials, respectively.

However, very little is known about the mechanism of the radiation detection, except for the basic principle, as described above. Thus, studies on the creation of ultra-high-accuracy detectors have primarily followed empirically observed rules. In order to aid researchers engaging in measurement and experimentation and contribute to detector development in general, the materials simulator developer team of CCSE has attempted to develop a method of predicting detection processes via simulation [1.4.1-1 through 1.4.1-5]. In the developed simulation, an equation expressing the superconducting transition dynamics near the transition point, the heat diffusion, and the Maxwell equations describing the heat transfer and the subsequent creation of the electrical signal are solved together. Thus, the code [1.4.1-6 through 1.4.1-9] can reproduce the detection process via the superconductivity depression by the heat diffusion (Fig. 1.4.1-1).

In fiscal year 2006, by utilizing the developed simulation code, we performed a simulation for neutron detection of the superconductor MgB_2 [1.4.1-10 through 1.4.1-13] and predicted the detector performance prior to experiments. First, we revealed that the response time is on the order of one nanosecond, and the experiments in JRR-3 confirmed the prediction to be valid. Thus, the simulation code is shown to work well, and the response speed is much faster than that of the previous detectors. This indicates that MgB_2 has good potential as an ultra-accurate neutron detector. At present, further experiments and simulations are underway.

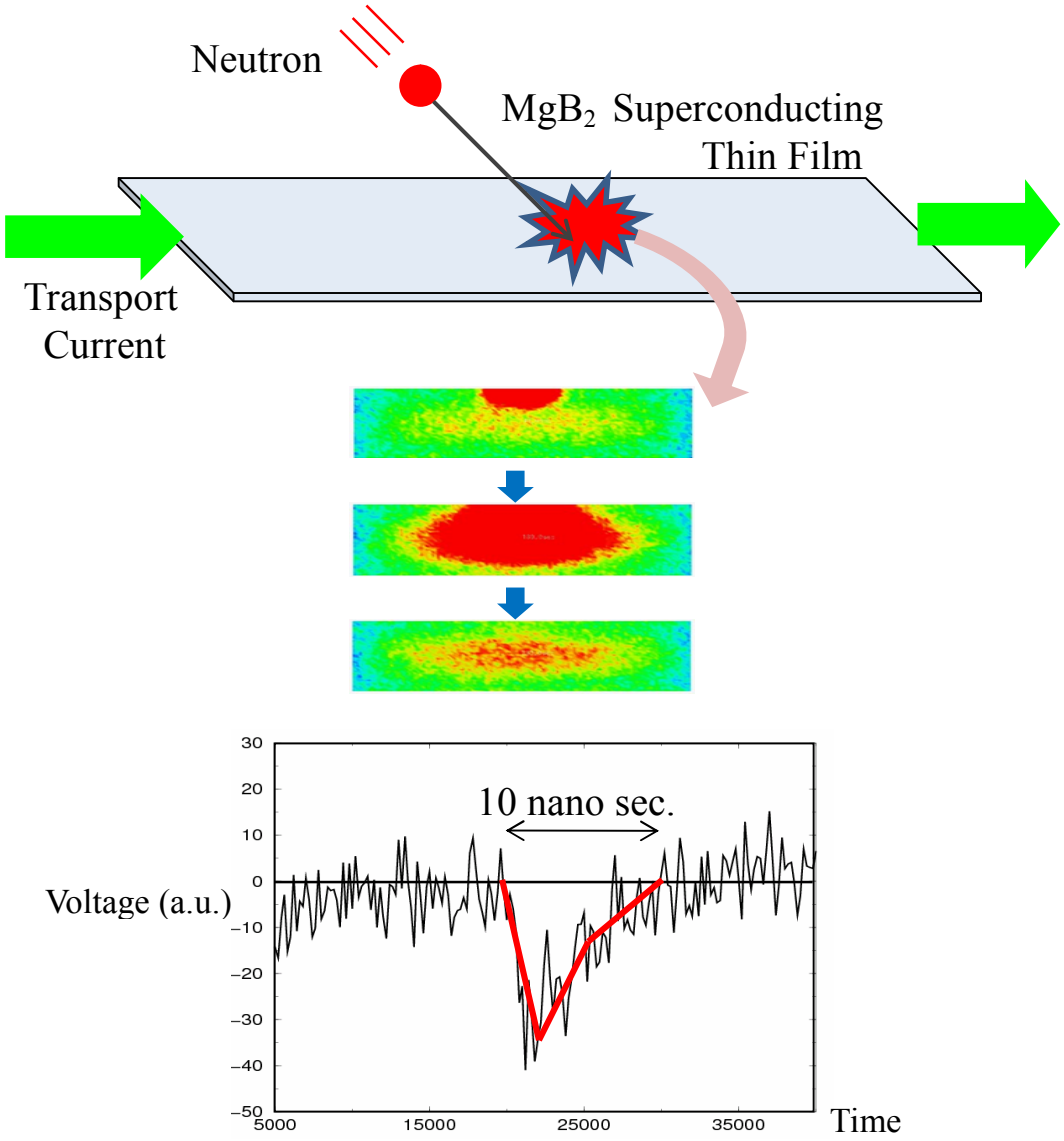

Fig. 1.4.1-1. The transport current is applied on MgB_2 superconducting thin film (top panel). Then, if a neutron hits the film and a nuclear reaction occurs, the reaction heat energy depresses the superconductivity and produces a resistance enhancement. In this situation, we predict the time development of the voltage signal as shown in the bottom panel via the numerical simulations, for which three time snapshots of the superconducting electron density profile are displayed in the middle panel.

1.4.2 Simulation of Crack Propagation speed in Stress Corrosion Cracking

Estimation of crack speed is essential for safety assessment of structural materials. The speed depends on the material and the applied tensile stress, as well as the environment, and, usually, a formula that is obtained from experiments is used to estimate crack speed in the operational condition. In the case of stainless steel inside a nuclear reactor, the material is subjected to hot coolant water and cracks initiated at a far lower stress compared to the normal environment. This phenomenon is referred to as stress corrosion cracking (SCC), for which safety assessment becomes more subtle. Unfortunately, the exact mechanism of SCC remains unclear, and currently there is no sufficiently clear theoretical explanation of the crack-speed formula for SCC. In the present study, we attempt to develop a modeling for SCC, which can reproduce the experimentally observed crack speed and provide a possible theoretical explanation of the crack-speed formula.

Our modeling is based on an assumption regarding the SCC process inferred from experimental observations, namely, a rich amount of oxygen is usually observed in the grain boundaries ahead of the crack tips. These grain boundaries are oxidized and become far more brittle than the normal boundaries. Thus, we have speculated the SCC process to be as follows: (1) a grain boundary next to the crack tip is opened a small amount owing to tensile stress concentration, and becomes a diffusion channel for oxygen atoms, (2) oxygen atoms from the corrosive environment rapidly diffuse through this grain boundary, making it brittle, and (3) the brittle oxidized grain boundary fails and failure stops at grain boundary triple junction, owing to crack tip blunting caused by grain boundary slide. Based on these assumptions, we modeled the SCC process as successive failures of an embrittled grain boundary next to a crack tip.

We have constructed a simulation sample consisting of 1,000 crystal grains of randomly oriented crystal axes with the elastic constants of iron. The geometry of grain boundaries was generated by random Voronoi decomposition. The initial crack was introduced to allow stress concentration, and tensile stress was applied to the sample. The stress distribution in the sample was calculated by the finite element method using tetrahedral elements, as shown in Fig. 1.4.2-1.

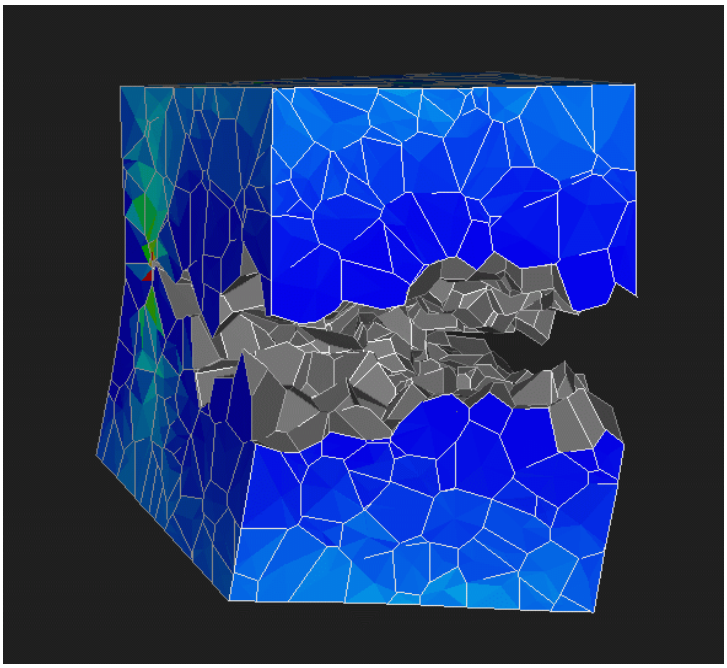

Fig. 1.4.2-1. Three-dimensional visualization of modeled geometry of grain boundaries and stress distribution. The colors indicate the strength of the local tensile stress.

The crack propagation is modeled as follows. When the local tensile stress acting on a grain boundary exceeds a fracture threshold, that grain boundary fails and the crack proceeds along this boundary, the stress distribution is then re-calculated and the process is repeated. The embrittlement effect of oxygen is incorporated into the model via the change of the fracture threshold. The concentration of oxygen atoms in each grain boundary is updated in each time step, and so is the fracture threshold of each grain boundary. In the present study, we assumed that the fracture threshold stress decreases to one tenth the normal value when the oxygen concentration is saturated, and at the intermediate concentration, the threshold is linearly interpolated. Furthermore, we have assumed that the rate of increase of the oxygen concentration C on a grain boundary adjacent to a crack tip is proportional to some power of the tensile stress σ acting on that grain boundary, as follows:

$$dC/dt = A\,\sigma^{n},$$

where A is a constant to be fitted to the actual experimental data and n is the exponent of the power. Figure 1.4.2-2 shows the crack propagation speed plotted with respect to tensile stress applied to the system for two cases, namely, n = 2 and n = 1/2. We have found that the case of n = 2 reproduces the qualitative features of the experimentally

observed data. An improved model, which incorporates the results of quantum mechanical calculation on the embrittlement effect of oxygen and uses a more realistic diffusion calculation of oxygen concentration, is currently being developed.

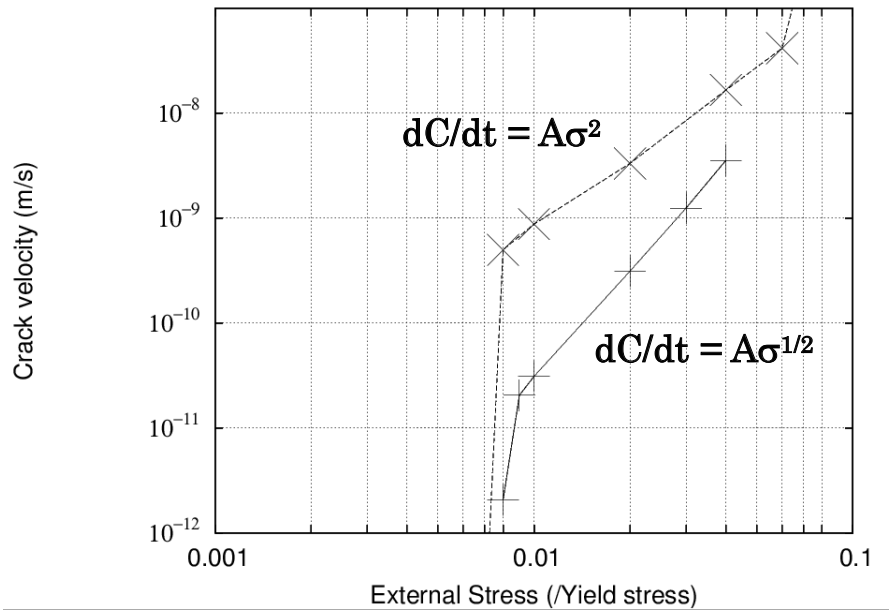

Fig. 1.4.2-2. Crack propagation speed plotted against tensile stress applied to the system for two cases, n = 2 and n = 1/2.

1.4.3 Mesoscale modeling of the rim-structure formation of UO_2 fuel pellets

The thermal and mechanical properties of uranium-dioxide (UO_2) fuel have been studied in order to realize safer and more economic operation of nuclear power plants. An important safety-related requirement is to confine the highly-radioactive fission products within the fuel pellet. However, it is known that a typical microstructural change occurs at the peripheral region of fuel pellets over some critical value of the burnup ~60 MWd/kgU, that is, nano-sized bubbles containing fission-gas atoms such as Xe atoms aggregate and form large bubbles with a diameter of ~2 μm. At the same time, the original grains become subdivided. See the SEM micrograph shown in Fig. 1.4.3-1. These changes might promote the swelling of the pellet and gas-release, both of which are not desirable for safe operation.

The bubble formation and the grain sub-division occur at almost the same time, it is therefore considered that the phenomena are closely related. Since the sub-divided grains have few defects, the UO_2 crystal undergoes a type of "restructuring", and the inert gas atoms aggregate during the "restructuring" process. A clear view of the mechanism of these changes has been sought for more than 20 years, but there is no definite consensus among the researchers.

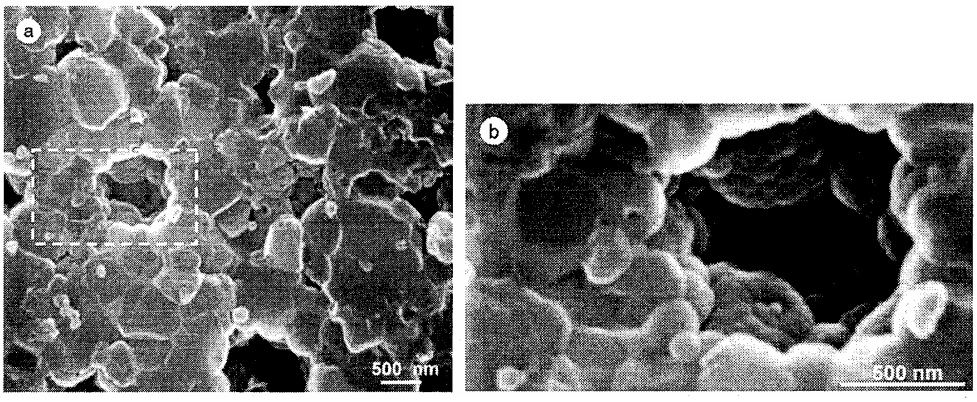

Fig. 1.4.3-1. SEM micrographs of the sample of 75 MWd/kgU, 1,000°C, showing (a) polyhedral grains away from the pore inner surface and (b) a high magnification image of the area surrounded by the white dashed line in (a), showing rounded grains inside a pore. From [1.4.3-1].

Last year we have developed a tool to simulate bubble development in the grain interior. In order to simulate the formation of the rim-structure, however, a tool to pursue the bubble development in the presence of grain boundaries is necessary. Here we discuss the development of gas bubbles at grain boundaries using a newly-devised mesoscale computer model. This model uses a Monte-Carlo simulation method that adopts a three-dimensional lattice system for the physical space. Each small lattice element carries variables that determine its state. The state of each element assumes either a bubble or a matrix state. A calculation element with the bubble state represent a cluster composed of vacancies and inert gas atoms. The inert gas considered herein is Xe. A calculation element with the matrix state also carries the state of its crystallographic orientation.

The dynamics of the model is determined by a series of Monte-Carlo steps, for which the Metropolis algorithm was adopted. The Hamiltonian used for the algorithm is composed of two types of energy: the grain boundary energy (E_{gb}) and bubble/matrix interface energy (E_{bm}). For E_{gb}, the Read-Shockley function [1.4.3-2] is used:

$$E_{gb} = \begin{cases} E_1(\theta/\theta_1)[1-\ln(\theta/\theta_1)] & \theta < \theta_1 \\ E_1 & \theta \geq \theta_1 \end{cases},$$

where $\theta = 15^{\circ}$. The relative values of the two types of energy were fixed throughout the present study as they satisfy E_{bm}: E_1 = 2:1. Their absolute values can be controlled by changing the Monte-Carlo temperature. The flip used in the Monte-Carlo algorithm is the migration of a bubble element. Therefore, the total number of bubble elements is conserved throughout the calculation.

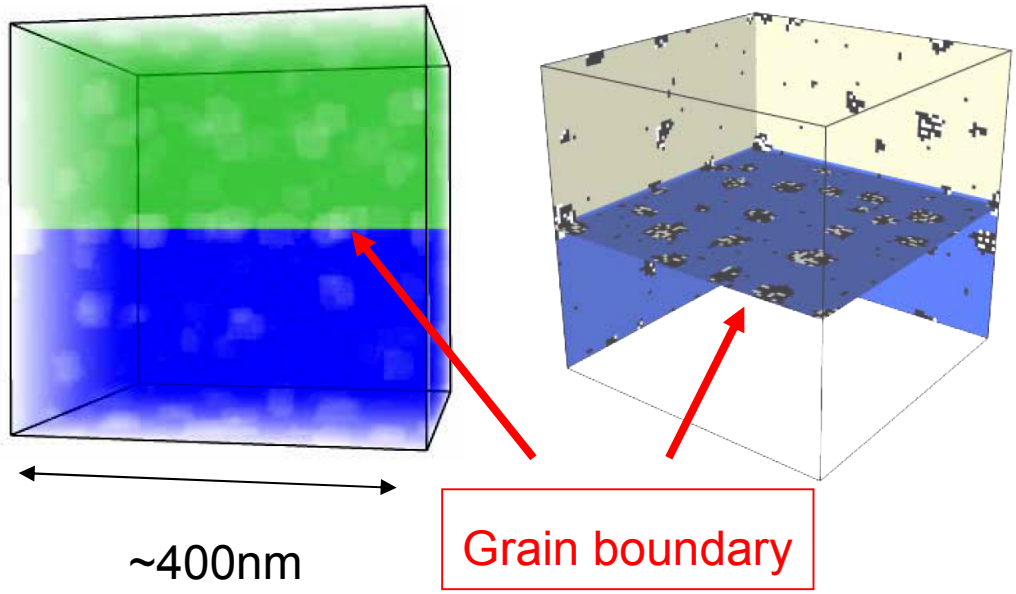

(a) (b)

Fig. 1.4.3-2. (a) Calculation results of bubble development, where developed bubbles are indicated by white transparent regions, and (b) the cross section at a grain boundary.

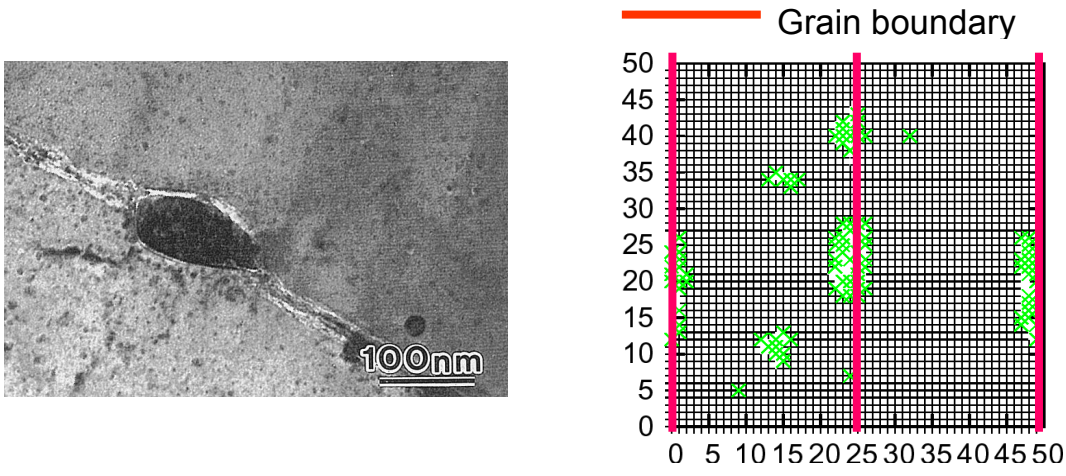

(a) (b)

Fig. 1.4.3-3. Comparison between an experimental results [3] (a) and calculation results (b).

A typical result starting from a random configuration of bubble elements is shown in Fig. 1.4.3-2 [1.4.3-4]. Figure 1.4.3-3 also shows the comparison between the

observed and calculated microstructures, both of which represent lenticular bubbles at the grain boundaries. This agreement suggests that the modelling here is successful.

In addition to the above study, we investigated the state of interstitial oxygen atoms. The rim structure formation in UO_2 fuel might be triggered by planar clusters of interstitial oxygen atoms. To clarify this possibility, we performed Monte-Carlo simulation of interstitial oxygen atom diffusion. Since the formation of a cluster of charged atoms requires a fair amount of Coulomb repulsion energy, there should be another type of interaction that overcomes the repulsion (although the charge of an interstitial oxygen atom depends on its circumstance, it should remain a finite value). As a possible mechanism for the cluster formation, we have selected the effect of lattice distortion, i.e., the oxygen atom at a lattice site is slightly displaced by the neighbouring interstitial oxygen atom. There are four possible neighbouring interstitial sites and the displacement was calculated in advance for each possible case (see Fig. 1.4.3-4). Using the above displacement values, the distortion energy values caused by the oxygen interstitials were calculated. Finally, the Monte-Carlo simulation for the migration of interstitial oxygen atoms was conducted using the energy values. In the calculation results, however, no planar cluster of interstitial oxygen atoms was observed, which suggests that the distortion effect is not large enough for the oxygen atoms to cluster.

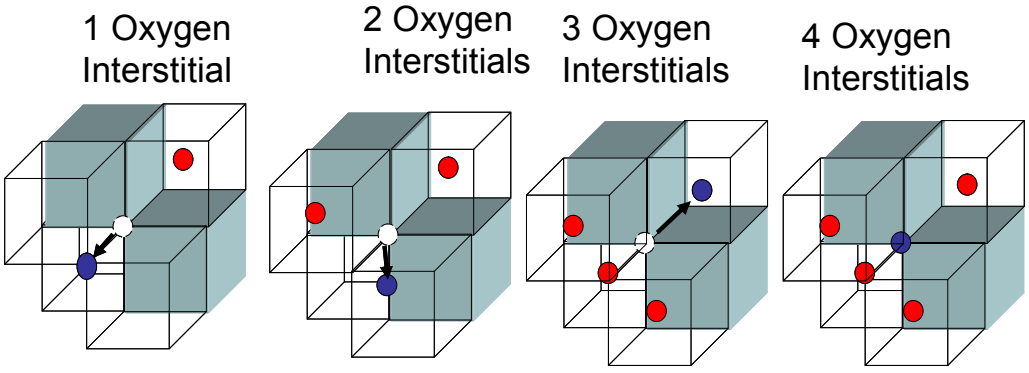

Fig. 1.4.3-4. Interstitial oxygen-sites (red circles) and displaced oxygen atoms (blue circles) from the lattice site.

References

[1.4.1-1] “Experimental and theoretical studies of d-dot” , Takekazu Ishida, Masaki Fujii, Taiji Abe, Masuo Yamamoto, Shigehito Miki, Shuichi Kawamata, Kazuo Satoh, Tsutomu Yotsuya, Masaru Kato, Masahiko Machida Physica C 437-438, pp.104-110 (2006).
[1.4.1-2] “A d-dot As an Element of Superconducting Devices”, M.Kato, H.Suematsu, M.Hirayama, T.Koyama, M.Machida, and T.Ishida, J.Korean Phys. Soc. 48, pp.1074-1079 (2006).
[1.4.1-3] “Experimental and Theoretical Studies of d-dot”,T.Ishida, M.Fujii, T.Abe, M.Yamamoto,S.Miki,S.Kawamata,K.Satoh, T.Yotsuya, M.Kato, M.Machida, Physica C437-438, pp.104-110 (2006).
[1.4.1-4] “Quasi-particle Spectrum of the Nano-scaled Anisotropic Superconducting Plate”,M.Kato, H.Suematsu, M.Machida, T.Koyama, and T.Ishida, Physica C437-438, pp.132-135 (2006).
[1.4.1-5] “A d-dot as an Element of Superconducting Devices”, M.Kato, H.Suematsu, M.Hirayama, T.Koyama, M.Machida, and T.Ishida, J. Korean Phys. Soc. 48, pp.1074-1079 (2006).
[1.4.1-6] “Time-dependent Ginzburg-Landau Theory for Atomic Fermi Gases near BCS-BEC Crossover”, M.Machida and T.Koyama, Phys. Rev. A74, 033603(2006).
[1.4.1-7] “Microscopic Structure of a Quantized Vortex Core in Atomic Fermi Gases”, M.Machida, Y.Ohashi, and T.Koyama, Phys. Rev. A74, 023621(2006).
[1.4.1-8] “Vortex Structure from BCS to BEC Superfluid”, M.Machida, T.Koyama, and Y.Ohashi, Physica C437-438, pp.190-194 (2006).
[1.4.1-9] “Effects of Edge Boundaries on Josephson Vortices in Finite-Size Layered High-Tc Superconductors”, M.Machida, Phys. Rev. Lett. 96, 097002 (2006)
[1.4.1-10] “Superconduction MgB_2 Films as Radiation Detectors”, T.Ishida, D.Fujiwara, M.Nishikawa, S.Miki, H.Shimakage, Z.Wang, K.Sato, T.Yotsuya, M.Machida, M.Kato, J.Korean Phys. Soc. 48, pp.1026-1031(2006).
[1.4.1-11] “Thermal Transient Response of Memberane-structured-superconducting MgB_2 Detector by Using 20-ps Pulse Laser”, T.Ishida, D.Fujiwara, S.Miki, H.Shimakage, Z.Wang, K. Satoh, T.Yotsuya, M.Machida, M.Kato, Nucl.Inst.Methods in Phys. Res. A 559, pp.582-584 (2006).
[1.4.1-12] “Direct Numerical Simulation on Non-equilibrium Superconducting Dynamics after Neutron Capture in MgB_2 Superconductor”, M.Machida, T.Koyama, M.Kato, and T.Ishidat, Nucl.Inst.Methods in Phys. Res. A 559, pp.594-596 (2006).

[1.4.1-13] “Superconducting MgB_2 Films as Radiation Detectors”, T.Ishida, D.Fujiwara, M.Nishikawa, S.Miki, H.Shimakage, Z.Wang, K.Sato, T.Yotsuya, M.Kato, and M.Machida, Physica C48, pp.1026-1028 (2006).
[1.4.2-1] M.Itakura, H.Kaburaki, and C.Arakawa, Phys. Rev. E **71**, 055102 (2005).
[1.4.3-1] T. Sonoda et al., Nucl. Inst. and Meth. In Phys. Res. B **191**, pp.622-628 (2002).
[1.4.3-2] W. T. Read, W. Shockley, Phys. Rev. **78**, pp.275-289(1950).
[1.4.3-3] K. Nogita, K. Une, J. Nucl. Mat. **226**, pp.302-310(1995).
[1.4.3-4] T. Suzudo, M. Itakura, Y. Fukuda, H. Kaburaki, “A Three-Dimensional Computer Modeling on the Development of Bubbles in Polycrystalline Materials”, Third International Conference Multiscale Materials Modeling, September, 2006, Freiburg, Germany.

2. Publication & Presentation List

List of Paper

1) A. Nishida, “Wave propagation properties of frame structures – Formulation for three-dimensional frame structures,” JSME International Journal Series B **49**, “*Special Issue on International Conferences on Power and Energy*,” 360 (2006).
2) R. Tian, H. Matsubara, and G. Yagawa, “Advanced 4-node tetrahedrons,” *Int. J. Numer. Meth. Engng.* **68**, 1209 (2006).
3) R. Tian and G. Yagawa, “Allman’s triangle, rotational DOF and partition of unity,” *Int. J. Numer. Meth. Engng.* **69**, 837 (2007).
4) M. Ida, T. Naoe, and M. Futakawa, “Direct observation and theoretical study of cavitation bubbles in liquid mercury,” *Physical Review E* **75**, 046304 (2007).
5) N.Nakajima, A.Miyazaki, Y.Suzuki, H.Matsubara, O.Hazama, F.Araya, Y.Kushida, K.Kawasaki, M.tani, N.Nakajima, A.Nishida, Y.Suzuki, H.Matsubara, O.Hazama, N.Kushida, and K.Kawasaki, "A METHODOLOGY OF STRUCTURAL ANALYSIS FOR NUCLEAR POWER PLANT SIZE OF ASSEMBLY", *Proceedings of International Conference on Supercomputing in Nuclear Applications* (SNA 2007) (CD-ROM).
6) Y.Suzuki, N.Matsumoto, Y.Idomura, and M.Tani, "Visualization System for Grid Environment in the Nuclear Field", *Proceedings of 34th Visualization Symposium* **26** Suppl. No.1 pp.49-52 (2006).
7) F.Araya, T.Hirayama, N.Nakajima, "Deployment of Computational Science in JAEA", *Atomic Energy Eye* Vol.52 23－34.
8) Y.Suzuki ; T.Aoyagi, M.Tani, N.Nakajima, T.Hirayama, "Research and development of grid computing in Center for Computational Science and E-systems of Japan Atomic Energy Agency", *Atomic Energy Eye*, Vol.52 pp.35-39
9) Ishida, H., Matsumoto, A., Tsutsumi, Y., and Yura, K. Conformational analysis of the structure of ribosome fit into electron microscopy density maps with normal mode analyses and molecular dynamics simulations, *The proceedings of the 16th International Microscopy Congress,* p242 (2006).
10) Yura, K., Yamaguchi, A., Go, M. Coverage of whole proteome by structural genomics observed through protein homology modeling database. *J. Str. Func. Genomics*, 7 (2), 65-76 (2006).
11) Kim, T.P.O., Yura, K., Go, N. Amino acid residue doublet propensity in the protein-RNA interface and its application to RNA interface prediction. *Nucleic Acids*

Research, **34** (22), 6450-6460 (2006)

12) Yura, K., Shionyu, M., Hagino, K., Hijikata, A., Hirashima, Y., Nakahara, T., Eguchi, T., Shinoda, K., Yamaguchi, A., Takahashi, K., Itoh, T., Imanishi, T., Gojobori, T., Go, M. Alternative splicing in human transcriptome: functional and structural influence on proteins. *Gene*, **380** (2), 63-71 (2006).

13) Takeda, J., Suzuki, Y., Nakao, M., Barrero, R., Koyanagi, K., Jin, L., Motono, C., Hata, H., Isogai,T., Nagai, K., Otsuki, T., Kuryshev, V., Shionyu, M., Yura, K., Go, M., Thierry-Mieg, J., Thierry-Mieg, D., Wiemann, S., Nomura, N., Sugano, S., Gojobori, T., Imanishi, T. Large-scale identification and characterization of alternative splicing variants of human gene transcripts using 56,419 completely sequenced and manually annotated full-length cDNAs. *Nucleic Acids Research*, **34** (14), 3917-3928 (2006).

14) Matsumoto, A. & Olson, W. Predicted Effects of Local Conformational Coupling and External Restraints on the Torsional Properties of Single DNA Molecules. *Multiscale Modeling and Simulation* **5**, 1227-1247 (2006).

15) Yonetani, Y. Liquid water simulation: A critical examination of cutoff length, *J.Chem. Phys.*, **124**, 204501 (2006).

16) Yonetani, Y., Kono, H., Fujii, S., Sarai, A. and Go, N. DNA deformability and hydration studied by molecular dynamics simulation, *Mol. Sim.*, **33**, 103-107 (2007).

17) M. Machida, S. Yamada, Y. Ohashi, and H. Matsumoto, "On-site pairing and microscopic inhomogeneneity in confined lattice fermion systems" *Physical Review A* **74**, 053621 (2006).

18) M. Machida, and T. Koyama, "Microscopic Structure of a Quantized Vortex Core in Atomic Fermi Gases", *Phys. Rev. A* **74**, 033603 (2006).

19) M. Machida, "Time-Dependent Ginzburg-Landau Theory for Atomic Fermi Gasses near the BCS-BEC Crossover", *Phys. Rev. A* **74**, 023621 (2006).

20) K. Ebihara, and H. Kaburaki, "Lattice Boltzmann Simulation of Solution Chemistry for Crevice Corrosion", *Mathematics and Computers in Simulation* **72**, 117-123 (2006).

21) K. Ebihara, T. Suzudo, H. Kaburaki, and K. Takai, "Simulation of Separation of Hydrogen Desorption Peak for Grain Boundary", *Current Advances in Materials and Processes* **20**, 1259 (2007).

22) S. Yamada, T. Imamura, and M. Machida, "Preconditioned Conjugate Gradient Method for Large-scale Eigenvalue Problem of Quantum Problem: Convergence Property of Adaptive-shift Preconditioner", *Transactions of JSCES*, 20060027 (2006).

23) M. Yamaguchi, T. Shiga, and H. Kaburaki, "Grain boundary decohesion by sulfur segregation in ferromagnetic iron and nickel - A first-principles study" *Materials Transactions* **47**, 2682 (2006).
24) Li. Ju, F. Shimizu, and S. Ogata, "Yield Point of Metallic Glass", *Acta Materialia* **54**, 4293--4298 (2006).
25) T. Kadoyoshi, H. Kaburaki, F. Shimizu, H. Kimizuka , S. Jitsukawa, and Li Ju, "Molecular dynamics study on the formation of stacking fault tetrahedra and unfaulting of Frank loop in fcc metals", *Acta Materialia* **55** 3073 (2007).
26) F. Shimizu, Li. Ju, and S. Ogata, "Theory of Shear Banding in Metallic Glass and Molecular Dynamics Calculations", *Materials Transactions* **48**-11, 2923-2927 (2007).
27) M. Machida, and T. Koyama, "Collective Dynamics of Macroscopic Quantum Tunneling in Layered High-Tc Superconductors", *Supercond. Sci. Technol.* **20** S23-S27 (2007).
28) M. Machida, and T. Koyama, "Collective Macroscopic Tunneling in Intrinsic Josephson Junctions", *Physica C* **460-462**, 1321-1322 (2007).
29) M. Machida, Y. Ohashi, and T. Koyama, "Vortex Microscopic Structure in BCS to BEC Fermi Superfluids", *Physica C* **437-438**, 190-194 (2006).
30) S. Yamada, M. Machida, Y. Ohashi, and H. Matsumoto, "Strong Pairing and Microscopic Inhomogeneity of Lattice Fermion Systems", *Physica C* **445-448** 90-93 (2006).
31) M. Yamaguchi, H. Nishiyama, T. Shiga, H. Kaburaki, and H. Matsuzawa, "Impurity-induced decohesion in iron grain boundary - A first-principles study", *Proceedings of Multiscale Materials Modeling Conference 2006* (2006).

List of Research Report and Book

1) F. Araya, T. Hirayama, and N .Nakajima, “Deployment of Computational Science in JAEA,” *Nuclear Viewpoints* (*Genshiryoku Eye*) **52**, 22 (2006) [in Japanese].
2) Yonetani, Y. “On the treatment of long-range electrostatic interactions in biomolecular simulations”, *Frontiers of Computational Science* (eds. Y. Kaneda, H. Kawamura and M. Sasai), Springer, 209-214 (2007).
3) Go, M., Yura, K., Shionyu, M. “Contribution of computational biology and structural genomics to understand genome and transcriptome”, *Proceedings of the International Symposium on Frontiers of Computational Science 2005 (ISFCS2005)*, (eds. Y. Kaneda, H. Kawamura and M. Sasai), Springer, 75-80 (2007).
4) Yura, K.,"Encyclopedia of Bioinformatics” (Item: Biomolecule, DNA, RNA,Pprotein,

Contact map, Conformation change in protein, Combinatorial extension, DALI) .

List of Oral Presentation

1) A. Nishida, "A study on the wave propagation property of a 3D frame structure － Introduction of the Timoshenko beam theory," *Proceedings of 52nd Symposium on Structural Engineering*, (Tokyo, Japan, April 2006).
2) A. Nishida, "Wave propagation behavior of a multi-connected structure," *Proceedings of 13th International Congress on Sound and Vibration (ICSV-13)* (Vienna, Austria, July 2006).
3) Y. Suzuki, N. Kushida, N. Yamagishi, T. Minami, N. Matsumoto, K. Nakajima, H. Matsubara, R. Tian, O. Hazama, T. Aoyagi, M. Tani, and N. Nakajima, "Concept of a quake-proof information control and management system for nuclear power plant. Part 1: Construction of Atomic Energy Grid InfraStructure (AEGIS)," *2006 Fall Meeting of Atomic Energy Society of Japan*, (Sapporo, Japan, Sep. 2006).
4) A. Nishida, Y. Suzuki, H. Matsubara, R. Tian, O. Hazama, M. Tani, and N. Nakajima, "Concept of a quake-proof information control and management system for nuclear power plant. Part 2: Construction of three dimensional virtual vibration testbed by using Assembly Structure Analysis," *2006 Fall Meeting of Atomic Energy Society of Japan*, (Sapporo, Japan, Sep. 2006).
5) A. Nishida and H. Tsuru, "The effect of Timoshenko's coefficient on wave propagation analysis of beams," *The 56th National Congress of Theoretical and Applied Mechanics*, (Tokyo, Japan, March 2007).
6) A. Nishida and H. Tsuru, "Applicability of Timoshenko coefficient in impulsive analysis of a piping system structure," *2007 Annual Meeting of Atomic Energy Society of Japan*, (Nagoya, Japan, March 2007).
7) M. Ida, "On the effects of bubble-bubble interaction," *The 13th Symposium on Cavitation*, (Sapporo, Japan, June 2006).
8) M. Ida and N. Oshima, "On the numerical instability of the filtered Navier-Stokes equations," *Proceedings of the Conference on Computational Engineering and Science* **11**, (Osaka, Japan, June 2006).
9) Y. Idomura, M. Ida, S. Tokuda, and L. Villard, "Conservative gyrokinetic Vlasov simulation using Morinishi scheme," *33rd EPS Conference on Plasma Physics*, (Roma, Italy, June 2006).
10) I. Shinohara, Y. Okuda, S. Ito, N. Nakajima, and M. Ida, "Shape optimization using an adjoint variable method in ITBL grid environment," *14th International Conference on Nuclear Engineering (ICONE-14)*, (Florida, USA, July 2006).
11) M. Ida, "A complementary study of phase properties and interaction force of

acoustically interacting bubbles," *Proceedings of 2006 Annual Meeting, Japan Society of Fluid Mechanics*, (Kyushu, Japan, Sep. 2006).

12) I. Shinohara, Y. Okuda, S. Ito, N. Nakajima, and M. Ida, "Duct shape optimization by using adjoint variable method," *The 2006 Annual Meeting of the Japan Society for Industrial and Applied Mathematics*, (Tsukuba, Japan, Sep. 2006).

13) Y. Idomura, M. Ida, and S. Tokuda, "Conservative gyrokinetic Vlasov simulation," *VLASOVIA 2006*, (Florence, Italy, Sep. 2006).

14) M. Ida, "On the transition frequencies of acoustically coupled gas bubbles," *The 2006 APS Division of Fluid Dynamics 59th Annual Meeting*, (Florida, USA, Nov. 2006).

15) Y. Idomura, M. Ida, S. Tokuda, and L. Villard, "Development of conservative gyrokinetic Vlasov code," *The 23rd Annual Meeting of the Japan Society of Plasma Science and Nuclear Fusion Research*, (Tsukuba, Japan, Nov. 2006).

16) I. Shinohara, Y. Okuda, S. Ito, N. Nakajima, and M. Ida, " Shape optimization using adjoint variable method for maximum lift," *Proceedings of the 20th Symposium on Computational Fluids Dynamics*, (Tokyo, Japan, Dec. 2006).

17) Y. Idomura, M. Ida, and S. Tokuda, "Conservative gyrokinetic full conservative gyrokinetic full-f Vlasov simulation," *JIFT 2007 Workshop on* "*Gyrokinetic Simulation of Ion and Electron Temperature Gradient-Driven Transport*," (CA, USA, Jan. 2007).

18) I. Shinohara, Y. Okuda, S. Ito, N. Nakajima, and M. Ida, "Minimization of the surface force of an object in an unsteady flow," *The 2007 Meeting of the Union of Research Activity Groups*, *JSIAM*, (Nagoya, Japan, March 2007).

19) M. Ida, Y. Idomura, and S. Tokuda, "Development of conservative gyrokinetic Vlasov code and its application to fusion plasma turbulence simulation," *The 22nd TSFD Symposium* "*Turbulence Simulation and Flow Design*," (Tokyo, Japan, March 2007).

20) M. Ida, M. Futakawa, H. Kogawa, H. Kimura, T. Naoe, and A. Bucheeri, "Computational science approaches to mercury cavitation －Towards an erosion mitigation technique using gas microbubbles," *2007 Annual Meeting of Atomic Energy Society of Japan*, (Nagoya, Japan, March 2007).

21) N. Kasahara and O. Hazama, "Large-scale transient thermal stress analysis of a steam-generator tubesheet," *The 15th CCSE Workshop*, (Ueno, Japan, March 2007).

22) R. Tian, "Part/component-based large-scale finite element analysis: discontinuous meshes stitching up," *Proceedings of WCCM VII*, (Los Angeles, USA, July 2006).

23) Y.Kushida, Y.Suzuki, T.Minami, N.Nakajima, K.Rainer, and B.Thomas, "Interoperability Establishment between UNICORE and ITBL", 9th HLRS MetaComputing and Grid Workshop (Germany, Stuttgart, Jul. 2006)

24) Y.Suzuki, "Visualization system on ITBL", *Network Visualization Seminar*, (Tokyo, Japan, Jan. 2007).

25) Y.Suzuki, Y.Kushida, N.Yamagishi, K.Nakajima, T.Minami, N.Matsumoto, T.Aoyagi, N.Nakajima, K.Iba , N.Hayashi, T.Ozeki, H.Nakanishi, Y.Nagayama, "Application of Atomic Energy Grid InfraStructure(AEGIS) to Nuclear Fusion Research", *2007 Annual meeting of The Atomic Energy Society of Japan* (Nagoya, Japan, Mar. 2007).

26) Y.Suzuki, Y.Kushida, H.Matsubara, K.Nakajima, M.Tani, A.Miyazaki, R.Tien, and O.Hazama, "Depolyment of Computational Science in Nuclear Engineering and Science with HPC and Network Technology", *International Conference for High Performance Computing, Networking, Storage and Analysis (SC06)*, (Tampa, USA, Nov. 2006).

27) M. Adachi, T. Tamata, , K. Sato, K. Yura, I. Narumi, and R. Kuroki, "Analyses in interaction between DNA and PprA of the novel DNA repair protein derived from Deinococcus radiodurans", *The 6th Annual meeting of the Protein Science Society of Japan*, (Kyoto, Japan, Apr.2006)

28) K. Yura, "Characteristics of subunit interactions in biological supramolecules", *The 6th Annual meeting of the Protein Science Society of Japan*, (Kyoto, Japan, Apr.2006)

29) Kim, K. Yura, and N. Go, "Structure-based bioinformatics analyses and a prediction method of protein-RNA interfaces", *20th IUBMB International Congress of Biochemistry and Molecular Biology and 11th FAOBMB Congress*, (Kyoto, Japan, Jun.2006)

30) M. Shionyu, K. Yura, A. Hijikata, T. Nakahara, K. Shinoda, A. Yamaguchi, K. Takahashi, and M. Go, "Systematic detection of protein regions affected by alternative splicing", *20th IUBMB International Congress of Biochemistry and Molecular Biology and 11th FAOBMB Congress,* (Kyoto, Japan, Jun.2006)

31) K. Yura, "Prediction of protein biological functions three-dimensional structure data-in he case of RNA binding proteins", *5 th MEXT protein 3000 Forum*, (Sendai, Japan, Jun.2006) (Invited)

32) K. Yura and M. Go, "Effect on protein three-dimensional structures of alternative splicing toward diversification of eukaryotic transcripts", *Society of Evolutionary Studies, Japan, Annual meeting 2006*, (Tokyo, Japan, Aug.2006)

33) Kim, K. Yura, and N. Go, "Computational analyses of amino acid residue propensity in protein-RNA interfaces and prediction methods for the interfaces", *Fifth East Asian Biophysics Symposium and 44th Annual Meeting of the Biophysical Society of*

Japan, (Okinawa, Japan, Nov.2006)

34) Matsumoto, and W.K. Olson, "Predicted Effects of Local Conformational Coupling and External Restraints on the Torsional Properties of Single DNA Molecules", *Fifth East Asian Biophysics Symposium and 44th Annual Meeting of the Biophysical Society of Japan*, (Okinawa, Japan, Nov.2006)

35) K. Nakamura, K. Yura, and N. Go, "Prediction of Metal-Binding Sites from High-Throughput Metalloproteomics Data", *Pacific Symposium on Biocomputing 2007*, (Wailea, Maui, USA, Jan.2007)

36) K. Yura, "Prediction of protein-RNA interfaces based on protein 3D structure and evolutionary conservation", *Frontier in Bioinformatics*, (Tokyo, Japan, Mar.2007)

37) Matsumoto, "Structural analysis of ribosome based on the elastic network normal mode analysis", *51st Biophysical Society Annual Meeting*, (Baltimore, USA, Mar.2007)

38) M. Yamaguchi, H. Nishiyama, and H. Kaburaki, "Decohesion of bcc Fe grain boundary by phosphorous segregation", *Workshop on Structural Materials of Light Water Reactor* (Sendai, Japan, Jan. 2007)

39) M. Yamaguchi, H. Nishiyama, T. Shiga, and H. Kaburaki, "The effects of various segregated soiuers on the embrittlement of bcc fe grain bonudaries by the first princles calculation", *Material Research Society Fall Meeting 2006*, (Boston, USA, Nov. 2006)

40) M. Machida, "Numerical Simulations for Abrikosov and Josephson Vortices", *Nanoscience and Engineering for Young Scientists* (Atagawa, Japan, Nov. 2006)

41) S. Ogata, F. Shimizu Li. Ju M. Sawada and Y.Shibuya, "Atomistic Study of Shear Deformation Behavior of Bulk Metallics Glass", *Materials Transactions 5th International Bulk Metallic Glasses Conference* (Awaji, Japan, Oct. 2006)

42) T. Suzudo, M. Itakura, H. Kaburaki, and E. Wakai "Three-dimensional meso-scale Monte-Carlo simulation of the growth of bubbles", *International Symposium of Fusion Reactor Materials Development*, (Tokyo, Japan, Jul. 2006)

43) T. Suzudo, H. Kaburaki, and M. Itakura, "Mesoscopic simulation of bubble behaviors", *2007 Annual meeting of The Atomic Energy Society of Japan*, (Nagoya, Japan, Mar. 2007)

44) T. Suzudo, H. Kaburaki, and M. Itakura, "Mesoscopic Simulation of Fuel-Material Behaviors under Irradiation -A Computer Modeling on the Bubble Growth in UO_2 Fuel", *New Crossover Project Workshop-3*, (Tokyo, Japan, Dec. 2006)

45) H. Kaburaki, "Molecular dynamics simulations for lattice defects", *The 55'th meeting of The Society of Materials Science* (Tokyo, Japan, Sep. 2006)

46) H. Kaburaki, T. Kadoyoshi, M. Itakura, M. Yamaguchi, T. Suzudo, and S. Jitsukawa, "Microscopic simulations on the hardening and embrittlement materials", *International Symposium on Fusion Reactor Materials Development* (Tokyo, Japan, Jul. 2006)

47) F. Shimizu, S. Ogata, and Li. Ju, "Large-Scale Molecular Dynamics Simulation of Shear Band Propagation in Metallic Glass", *The 50'th Japan Congress on Materials Research*, (Kyoto, Japan, Dec. 2006)

48) F. Shimizu, S. Ogata, M. Yamaguchi, T. Kano, and H. Kaburaki, "First-principles Calculation on Screw Dislocation Core Properties in BCC Metals", *2007 Annual meeting of The Atomic Energy Society of Japan*, (Nagoya, Japan, Mar. 2007)

49) Li. Ju, F. Shimizu, and S. Ogata, "Large-Scale Molecular Dynamics Simulation of Shear Band Propagation in Metallic Glass", *TMS (Minerals, Metals and Materials Society) 2007 Annual Meeting and Exhibition*, (Orlando, USA, Feb. 2007)

50) Li. Ju, F. Shimizu, and S. Ogata, "Size Effects in Metallic Glass", *2006 Materials Research Society (MRS) Fall Meeting*, (Boston, USA, Nov. 2006)

51) Li. Ju, F. Shimizu, and S. Ogata, "Yield Point of Metallic Glass", *TMS (Minerals, Metals and Materials Society) 2007 Annual Meeting and Exhibition*, (Orlando, USA, Feb. 2007)

52) T. Shiga, and N. Tachikawa, "Accelerating combined quantum mechanical/molecular mechanical molecular dynamics using multiple-time-scale approach combined with perturbation theory" (Yokohama, Japan, Jun. 2006)

53) T. Shiga, and N. Tachikawa, "ab initio QM/MM molecular dynamics by multiple-time-scale approach", *Symposium on Molecular Structure*, (Shizuoka, Japan, Sep. 2006)

54) T. Shiga, "Accelerating QM/MM molecular dynamics using multiple-time-scale approach and perturbation theory", *Gordon Research Conference (Computational Chemistry)*, (Les Diablerets, Switzerland Oct. 2006)

55) M. Yamaguchi, "First-principles study on grain boundary embrittlement", *2006 Annual Meeting of The Japan Institute of Metals*, (Niiata, Japan, Sep. 2006)

56) M. Yamaguchi, "First-principles study on the grain boundary embrittlement of metals", *2006 Annual meeting of The Atomic Energy Society of Japan*, (Nagoya, Japan, Mar. 2007)

57) M. Yamaguchi, H. Nishiyama, and H. Kaburaki, "Iron grain boundary decohesion by phosphorous segregation - A first-principles study", *The 13th Meeting of the International Group on Radiation Damage Mechanisms in Pressure Vessel Steels*, (Tsukuba, Japan, Oct. 2006)

58) M. Yamaguchi, T. Shiga, and H. Kaburaki, "First-principles study on the grain boundary embrittlement of metals", *2006 Annual meeting of The Atomic Energy Society of Japan*, (Sapporo, Japan, Sep. 2006)

59) S. Yamada, T. Imamura, and M. Machida, "Parallel Algorithm to Realize Huge-scale Matrix Diagonzalization Encountered in Quantum Many-body Problems: Current Status of Massively Parallel Calculation for Quantum Physics on the Earth Simulator", *RIMS Workshop*, (Kyoto, Japan, Nov. 2006)

60) S. Yamada, T. Imamura, T. Kano, and M. Machida, "High-Performance Computing for Exact Numerical Approaches to Quantum Many-Body Problems on the Earth Simulator", *Supercomputing 2006* (Tampa, USA, Nov. 2006)

61) M. Machida, "Confinement Effects for Josephson Vortices in Layered High-Tc Superconductors", *International Workshop on Mesoscopic Superconductivity and Magnetism*, (Chicago, USA, Aug. 2006)

62) M. Machida, and T. Koyama, "Macroscopic Quantum Tunneling in High-Tc Intinsic Josephson Junctions: Collective Phenomenon I", *The 2006 Annual Meeting of The Physical Society of Japan*, (Chiba, Japan, Sep. 2006)

63) M. Machida, S. Yamada, Y. Ohashi, and H. Matsumoto, "Inhomogeneous Ground State in Fermion Optical Lattice", *The 2006 Annual Meeting of The Physical Society of Japan*, (Chiba, Japan, Sep. 2006)

64) K. Ebihara, T. Suzudo, H. Kaburaki, and K. Takai, "Simulation of Separation of Hydrogen Desorption Peak for Grain Boundary", *The 154th ISIJ Meeting* (Gifu, Japan, Sep. 2007)

65) N. Sasa, "Nonlinear dynamics in an ultra cold atomic gas", *Workshop on Nonlinear Physics*, (Fukuoka, Japan, Nov. 2006)

3. Staff List of CCSE

Director:	Toshio Hirayama

Computer Science Research and Development Office

Division Leader:	Norihiro Nakajima
Principal Engineer:	Tetsuo Aoyagi
Principal Researcher:	Shinji Tokuda
Assistant Principal Researcher:	Fumimasa Araya
	Yoshio Suzuki
Assistant Principal Engineer:	Toshihiko Matsuura
Scientist:	Masato Ida
Staff (engineer):	Hideo Kimura
Collaborating Engineer:	Nobuko Matumoto
	Yukihiro Hasegawa
	Nobuhiro Yamagishi
	Takahiro Minami
	Kohei Nakajima
Senior Post-Doctor Fellow:	Osamu Hazama
	Akemi Nishida (Miyazaki)
	Rong Tian (until December 2006)
	Noriyuki Kushida
Post-Doctor Fellow:	Hitoshi Matsubara

Simulation Technology Research and Development Office

Division Leader:	Masahiko Machida
Vice Division Leader	Kei Yura
Invited Researcher:	Chuichi Arakawa
Assistant Principal Researcher:	Tomoaki Suzudo
	Masatake Yamaguch
	Mituhiro Itakura
	Motoyuki Siga
Scientist:	Narimasa Sasa
	Futoshi Shimizu

	Susumu Yamada
	Atushi Matumoto
	Ken-ichi Ebihara
Collaborating Engineer:	Tomoko Kadoyoshi
Senior Post-Doctor Fellow:	Kensuke Nakamura
Fellow of Advanced Science:	Masataka Oikawa
JST CREST Post-doctor Fellow	Yonetani Yoshiteru

This is a blank page.

国際単位系（SI）

表１．SI 基本単位

基本量	SI 基本単位	
	名称	記号
長さ	メートル	m
質量	キログラム	kg
時間	秒	s
電流	アンペア	A
熱力学温度	ケルビン	K
物質量	モル	mol
光度	カンデラ	cd

表２．基本単位を用いて表されるSI組立単位の例

組立量	SI 基本単位	
	名称	記号
面積	平方メートル	m^2
体積	立法メートル	m^3
速さ，速度	メートル毎秒	m/s
加速度	メートル毎秒毎秒	m/s^2
波数	毎メートル	m-1
密度（質量密度）	キログラム毎立法メートル	kg/m^3
質量体積（比体積）	立法メートル毎キログラム	m^3/kg
電流密度	アンペア毎平方メートル	A/m^2
磁界の強さ	アンペア毎メートル	A/m
（物質量の）濃度	モル毎立方メートル	mol/m^3
輝度	カンデラ毎平方メートル	cd/m^2
屈折率	（数の）1	1

表５．SI 接頭語

乗数	接頭語	記号	乗数	接頭語	記号
10^{24}	ヨタ	Y	10^{-1}	デシ	d
10^{21}	ゼタ	Z	10^{-2}	センチ	c
10^{18}	エクサ	E	10^{-3}	ミリ	m
10^{15}	ペタ	P	10^{-6}	マイクロ	μ
10^{12}	テラ	T	10^{-9}	ナノ	n
10^{9}	ギガ	G	10^{-12}	ピコ	p
10^{6}	メガ	M	10^{-15}	フェムト	f
10^{3}	キロ	k	10^{-18}	アト	a
10^{2}	ヘクト	h	10^{-21}	ゼプト	z
10^{1}	デカ	da	10^{-24}	ヨクト	y

表３．固有の名称とその独自の記号で表されるSI組立単位

組立量	SI 組立単位			
	名称	記号	他のSI単位による表し方	SI基本単位による表し方
平面角	ラジアン(a)	rad		$m \cdot m^{-1}=1$(b)
立体角	ステラジアン(a)	sr(c)		$m^2 \cdot m^{-2}=1$(b)
周波数	ヘルツ	Hz		s^{-1}
力	ニュートン	N		$m \cdot kg \cdot s^{-2}$
圧力，応力	パスカル	Pa	N/m^2	$m^{-1} \cdot kg \cdot s^{-2}$
エネルギー，仕事，熱量	ジュール	J	N・m	$m^2 \cdot kg \cdot s^{-2}$
工率，放射束	ワット	W	J/s	$m^2 \cdot kg \cdot s^{-3}$
電荷，電気量	クーロン	C		s・A
電位差（電圧），起電力	ボルト	V	W/A	$m^2 \cdot kg \cdot s^{-3} \cdot A^{-1}$
静電容量	ファラド	F	C/V	$m^{-2} \cdot kg^{-1} \cdot s^4 \cdot A^2$
電気抵抗	オーム	Ω	V/A	$m^2 \cdot kg \cdot s^{-3} \cdot A^{-2}$
コンダクタンス	ジーメンス	S	A/V	$m^{-2} \cdot kg^{-1} \cdot s^3 \cdot A^2$
磁束	ウエーバ	Wb	V・s	$m^2 \cdot kg \cdot s^{-2} \cdot A^{-1}$
磁束密度	テスラ	T	Wb/m^2	$kg \cdot s^{-2} \cdot A^{-1}$
インダクタンス	ヘンリー	H	Wb/A	$m^2 \cdot kg \cdot s^{-2} \cdot A^{-2}$
セルシウス温度	セルシウス度(d)	℃		K
光束	ルーメン	lm	cd・sr(c)	$m^2 \cdot m^{-2} \cdot cd=cd$
照度	ルクス	lx	lm/m^2	$m^2 \cdot m^{-4} \cdot cd=m^{-2} \cdot cd$
（放射性核種の）放射能	ベクレル	Bq		s^{-1}
吸収線量，質量エネルギー分与，カーマ	グレイ	Gy	J/kg	$m^2 \cdot s^{-2}$
線量当量，周辺線量当量，方向性線量当量，個人線量当量，組織線量当	シーベルト	Sv	J/kg	$m^2 \cdot s^{-2}$

(a)ラジアン及びステラジアンの使用は、同じ次元であっても異なった性質をもった量を区別するときの組立単位の表し方として利点がある。組立単位を形作るときのいくつかの用例は表４に示されている。
(b)実際には、使用する時には記号rad及びsrが用いられるが、習慣として組立単位としての記号“１”は明示されない。
(c)測光学では、ステラジアンの名称と記号srを単位の表し方の中にそのまま維持している。
(d)この単位は、例としてミリセルシウス度m℃のようにSI接頭語を伴って用いても良い。

表４．単位の中に固有の名称とその独自の記号を含むSI組立単位の例

組立量	SI 組立単位		
	名称	記号	SI 基本単位による表し方
粘度	パスカル秒	Pa・s	$m^{-1} \cdot kg \cdot s^{-1}$
力のモーメント	ニュートンメートル	N・m	$m^2 \cdot kg \cdot s^{-2}$
表面張力	ニュートン毎メートル	N/m	$kg \cdot s^{-2}$
角速度	ラジアン毎秒	rad/s	$m \cdot m^{-1} \cdot s^{-1}=s^{-1}$
角加速度	ラジアン毎平方秒	rad/s^2	$m \cdot m^{-1} \cdot s^{-2}=s^{-2}$
熱流密度，放射照度	ワット毎平方メートル	W/m^2	$kg \cdot s^{-3}$
熱容量，エントロピー	ジュール毎ケルビン	J/K	$m^2 \cdot kg \cdot s^{-2} \cdot K^{-1}$
質量熱容量（比熱容量），質量エントロピー	ジュール毎キログラム毎ケルビン	J/(kg・K)	$m^2 \cdot s^{-2} \cdot K^{-1}$
質量エネルギー（比エネルギー）	ジュール毎キログラム	J/kg	$m^2 \cdot s^{-2} \cdot K^{-1}$
熱伝導率	ワット毎メートル毎ケルビン	W/(m・K)	$m \cdot kg \cdot s^{-3} \cdot K^{-1}$
体積エネルギー	ジュール毎立方メートル	J/m^3	$m^{-1} \cdot kg \cdot s^{-2}$
電界の強さ	ボルト毎メートル	V/m	$m \cdot kg \cdot s^{-3} \cdot A^{-1}$
体積電荷	クーロン毎立方メートル	C/m^3	$m^{-3} \cdot s \cdot A$
電気変位	クーロン毎平方メートル	C/m^2	$m^{-2} \cdot s \cdot A$
誘電率	ファラド毎メートル	F/m	$m^{-3} \cdot kg^{-1} \cdot s^4 \cdot A^2$
透磁率	ヘンリー毎メートル	H/m	$m \cdot kg \cdot s^{-2} \cdot A^{-2}$
モルエネルギー	ジュール毎モル	J/mol	$m^2 \cdot kg \cdot s^{-2} \cdot mol^{-1}$
モルエントロピー，モル熱容量	ジュール毎モル毎ケルビン	J/(mol・K)	$m^2 \cdot kg \cdot s^{-2} \cdot K^{-1} \cdot mol^{-1}$
照射線量（X線及びγ線）	クーロン毎キログラム	C/kg	$kg^{-1} \cdot s \cdot A$
吸収線量率	グレイ毎秒	Gy/s	$m^2 \cdot s^{-3}$
放射強度	ワット毎ステラジアン	W/sr	$m^4 \cdot m^{-2} \cdot kg \cdot s^{-3}=m^2 \cdot kg \cdot s^{-3}$
放射輝度	ワット毎平方メートル毎ステラジアン	$W/(m^2 \cdot sr)$	$m^2 \cdot m^{-2} \cdot kg \cdot s^{-3}=kg \cdot s^{-3}$

表６．国際単位系と併用されるが国際単位系に属さない単位

名称	記号	SI 単位による値
分	min	1 min=60s
時	h	1h =60 min=3600 s
日	d	1 d=24 h=86400 s
度	°	1°=(π/180) rad
分	’	1’=(1/60)°=(π/10800) rad
秒	”	1”=(1/60)’=(π/648000) rad
リットル	l、L	1l=1 $dm^3=10^{-3}m^3$
トン	t	$1t=10^3$ kg
ネーパ	Np	1Np=1
ベル	B	1B=(1/2)ln10(Np)

表７．国際単位系と併用されこれに属さない単位でSI単位で表される数値が実験的に得られるもの

名称	記号	SI 単位であらわされる数値
電子ボルト	eV	$1eV=1.60217733(49) \times 10^{-19}J$
統一原子質量単位	u	$1u=1.6605402(10) \times 10^{-27}kg$
天文単位	ua	$1ua=1.49597870691(30) \times 10^{11}m$

表８．国際単位系に属さないが国際単位系と併用されるその他の単位

名称	記号	SI 単位であらわされる数値
海里		1海里=1852m
ノット		1ノット=1海里毎時=(1852/3600)m/s
アール	a	1 a=1 $dam^2=10^2m^2$
ヘクタール	ha	1 ha=1 $hm^2=10^4m^2$
バール	bar	1 bar=0.1MPa=100kPa=1000hPa=10^5Pa
オングストローム	Å	1 Å=0.1nm=10^{-10}m
バーン	b	1 b=100$fm^2=10^{-28}m^2$

表９．固有の名称を含むCGS組立単位

名称	記号	SI 単位であらわされる数値
エルグ	erg	1 erg=10^{-7} J
ダイン	dyn	1 dyn=10^{-5}N
ポアズ	P	1 P=1 dyn・s/cm^2=0.1Pa・s
ストークス	St	1 St =1$cm^2/s=10^{-4}m^2/s$
ガウス	G	1 G ^10^{-4}T
エルステッド	Oe	1 Oe ^(1000/4π)A/m
マクスウェル	Mx	1 Mx ^10^{-8}Wb
スチルブ	sb	1 sb =1$cd/cm^2=10^4cd/m^2$
ホト	ph	1 ph=10^4lx
ガル	Gal	1 Gal =1$cm/s^2=10^{-2}m/s^2$

表10．国際単位に属さないその他の単位の例

名称	記号	SI 単位であらわされる数値
キュリー	Ci	1 Ci=3.7×10^{10}Bq
レントゲン	R	1 R = 2.58×10^{-4}C/kg
ラド	rad	1 rad=1cGy=10^{-2}Gy
レム	rem	1 rem=1 cSv=10^{-2}Sv
X線単位		1X unit=1.002×10^{-4}nm
ガンマ	γ	1γ=1 nT=10^{-9}T
ジャンスキー	Jy	1 Jy=$10^{-26}W \cdot m^{-2} \cdot Hz^{-1}$
フェルミ		1 fermi=1 fm=10^{-15}m
メートル系カラット		1 metric carat = 200 mg = 2×10^{-4}kg
トル	Torr	1 Torr = (101 325/760) Pa
標準大気圧	atm	1 atm = 101 325 Pa
カロリー	cal	
ミクロン	μ	1 μ =1μm=10^{-6}m

（第７版，1998年改訂）